Structural Element
Stiffness, Mass, and Damping Matrices

CEE 541. Structural Dynamics
Department of Civil and Environmental Engineering
Duke University

Henri P. Gavin
Fall 2020

1 Preliminaries

This document describes the formulation of stiffness and mass matrices for structural elements such as truss bars, beams, plates, and cables(?). The formulation of each element involves the determination of gradients of potential and kinetic energy functions with respect to a set of coordinates defining the displacements at the ends, or nodes, of the elements. The potential and kinetic energy of the functions are therefore written in terms of these nodal displacements (i.e., generalized coordinates). To do so, the distribution of strains and velocities within the element must be written in terms of nodal coordinates as well. Both of these distributions may be derived from the distribution of internal displacements within the solid element.

1.1 Node Displacements, Shape Functions, Internal Strain, Virtual Internal Strain

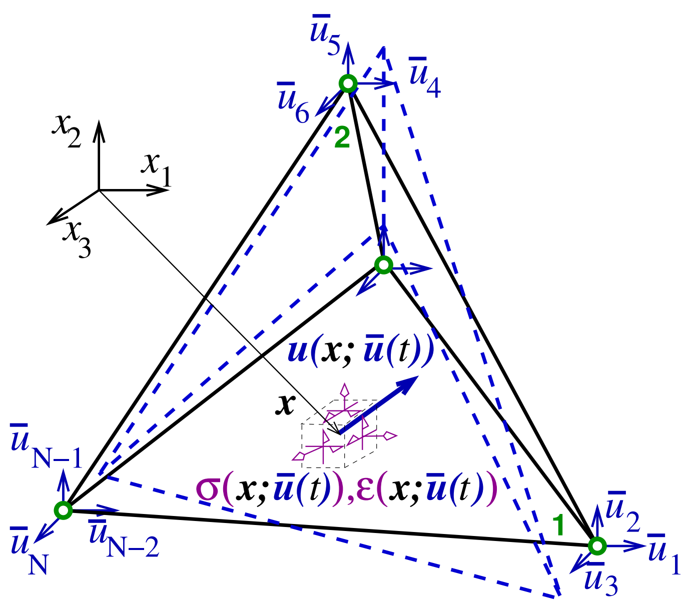

Figure 1. Displacements $\boldsymbol{u}$, strains $\boldsymbol{\epsilon}$, and stresses $\boldsymbol{\sigma}$ at a point $\boldsymbol{x}$ within a solid continuum can be expressed as a function of a set of time-dependent *nodal displacements* $\bar{\boldsymbol{u}}(t)$.

A component of a time-dependent displacement $u_i(\boldsymbol{x}, t)$, $(i = 1, \cdots, 3)$ in a solid continuum can be expressed in terms of the displacements of a set of nodal displacements, $\bar{u}_n(t)$ $(n = 1, \cdots, N)$ and a corresponding set of "shape functions" ψ_{in}, each relating coordinate displacement $\bar{u}_n(t)$ to internal displacement $u_i(\boldsymbol{x}, t)$.

$$u_i(\boldsymbol{x}, t) = \sum_{n=1}^{N} \psi_{in}(x_1, x_2, x_3)\ \bar{u}_n(t) \tag{1}$$

$$= \boldsymbol{\Psi}_i(\boldsymbol{x})\ \bar{\boldsymbol{u}}(t) \tag{2}$$

$$\boldsymbol{u}(\boldsymbol{x}, t) = [\boldsymbol{\Psi}(\boldsymbol{x})]_{3\times N}\ \bar{\boldsymbol{u}}(t) \tag{3}$$

Virtual displacements can make use of the same set of shape functions.

$$\delta u_i(\boldsymbol{x}, t) = \sum_{n=1}^{N} \psi_{in}(x_1, x_2, x_3)\ \delta\bar{u}_n(t) \tag{4}$$

$$= \boldsymbol{\Psi}_i(\boldsymbol{x})\ \delta\bar{\boldsymbol{u}}(t) \tag{5}$$

$$\delta\boldsymbol{u}(\boldsymbol{x}, t) = [\boldsymbol{\Psi}(\boldsymbol{x})]_{3\times N}\ \delta\bar{\boldsymbol{u}}(t) \tag{6}$$

Engineering strain, axial strain ϵ_{ii}, shear strain γ_{ij} are derived from partial derivitives (displacement gradients) of the displacement field. Note the "comma-notation" for partial derivitives, defined below.

$$\epsilon_{ii}(\boldsymbol{x}, t) = \frac{\partial u_i(\boldsymbol{x}, t)}{\partial x_i} \equiv u_{i,i}(\boldsymbol{x}, t) \tag{7}$$

$$\gamma_{ij}(\boldsymbol{x}, t) = \frac{\partial u_i(\boldsymbol{x}, t)}{\partial x_j} + \frac{\partial u_j(\boldsymbol{x}, t)}{\partial x_i} \equiv u_{j,i}(\boldsymbol{x}, t) + u_{i,j}(\boldsymbol{x}, t) \tag{8}$$

These partial derivitives in regular partial derivitive notation and in comma-notation are

$$\frac{\partial u_i(\boldsymbol{x})}{\partial x_j} = \sum_{n=1}^{N} \frac{\partial}{\partial x_j} \psi_{in}(x_1, x_2, x_3)\ \bar{u}_n(t) \tag{9}$$

$$u_{i,j}(\boldsymbol{x}) = \sum_{n=1}^{N} \psi_{in,j}(\boldsymbol{x})\ \bar{u}_n(t) \tag{10}$$

Strain-displacement relations relate the node displacements $\bar{u}_n(t)$ to the internal strains written with comma-notation as

$$\epsilon_{ii}(\boldsymbol{x}, t) = \sum_{n=1}^{N} \psi_{in,i}(\boldsymbol{x})\ \bar{u}_n(t) \tag{11}$$

$$\gamma_{ij}(\boldsymbol{x}, t) = \sum_{n=1}^{N} \left(\psi_{in,j}(\boldsymbol{x}) + \psi_{jn,i}(\boldsymbol{x})\right)\ \bar{u}_n(t) \tag{12}$$

Defining a Strain vector as a column vector of the elements of strain, all internal strains (and virtual strains) are linearly related to the node displacements through a matrix $\boldsymbol{B}_{\mathrm{e}}(\boldsymbol{x})$ which contains derivitives of the shape functions.

$$\boldsymbol{\epsilon}^{\mathsf{T}}(\boldsymbol{x}, t) \equiv \{\ \epsilon_{11}\ \ \epsilon_{22}\ \ \epsilon_{33}\ \ \gamma_{12}\ \ \gamma_{23}\ \ \gamma_{13}\ \} \tag{13}$$

$$\boldsymbol{\epsilon}(\boldsymbol{x}, t) = [\ \boldsymbol{B}_{\mathrm{e}}(\boldsymbol{x})\ ]_{6\times N}\, \bar{\boldsymbol{u}}(t) \qquad \text{and} \qquad \delta\boldsymbol{\epsilon}(\boldsymbol{x}, t) = [\ \boldsymbol{B}_{\mathrm{e}}(\boldsymbol{x})\ ]_{6\times N}\, \delta\bar{\boldsymbol{u}}(t) \tag{14}$$

1.2 Geometric Deformations in Slender Structural Elements

In slender structural elements, nonuniform transverse displacements ($u_{y,x}(x) \neq 0$) induce longitudinal deformations, $u_{x,x}(x)$. Longitudinal deformations arising from purely transverse displacements are called *geometric deformations*.

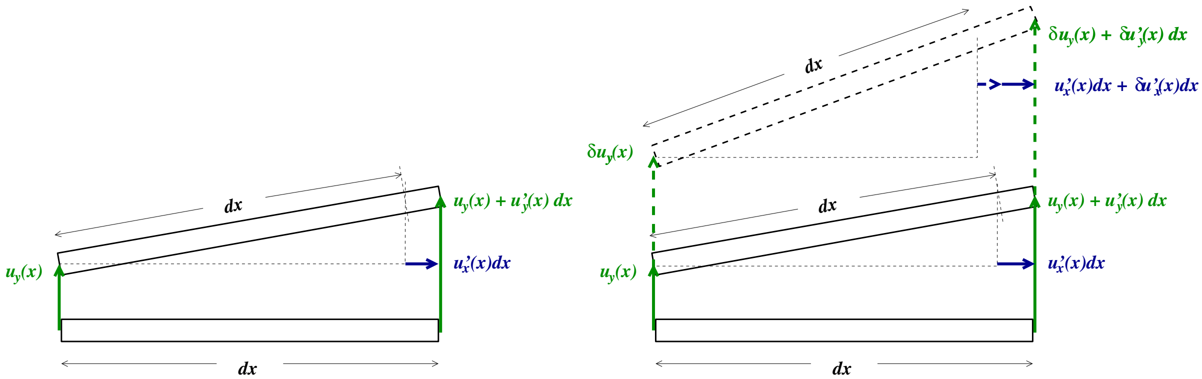

Figure 2. Transverse deformation $u_{y,x}(x)$ and axial geometric deformation $u_{x,x}(x)$ and virtual counterparts.

The Pythagorean theorem shows that geometric deformations are quadratic in $u_{x,x}(x)$ and $u_{y,x}(x)$.

$$\begin{aligned}
(dx - u_{x,x}(x)dx)^2 + (u_{y,x}(x)dx)^2 &= (dx)^2 \\
(1 - u_{x,x}(x))^2 + (u_{y,x}(x))^2 &= 1 \\
1 - 2u_{x,x}(x) + (u_{x,x}(x))^2 &= 1 - (u_{y,x}(x))^2 \\
2u_{x,x}(x) - (u_{x,x}(x))^2 &= (u_{y,x}(x))^2 \\
u_{x,x}(x) &= \frac{1}{2}(u_{x,x}(x))^2 + \frac{1}{2}(u_{y,x}(x))^2
\end{aligned}$$

Since slender structural elements are much more stiff in axial deformation than in transverse deformation, and since elastic tensile strains are limited to within 0.002 for most structural materials, $(u_{x,x})^2 < (0.002)^2 \ll (u_{y,x})^2$, the geometric portion of the deformation for slender structural elements is approximated as

$$u_{x,x}(x) \approx \frac{1}{2}(u_{y,x}(x))^2 \; . \tag{15}$$

With additional virtual displacements $\delta u_y(x)$, the virtual longitudinal deformation ($\delta u_{x,x}$) may also be analyzed using the Pythagorean theorem.

$$\begin{aligned}
(dx - u_{x,x}(x)dx - (\delta u_{x,x}(x))dx)^2 + (u_{y,x}(x) + (\delta u_{y,x}(x))dx)^2 &= (dx)^2 \\
(1 - u_{x,x} - \delta u_{x,x})^2 + (u_{y,x} + \delta u_{y,x})^2 &= 1 \\
1 - 2u_{x,x} - 2\delta u_{x,x} + (u_{x,x})^2 + 2(u_{x,x})(\delta u_{x,x}) + (\delta u_{x,x})^2 + (u_{y,x})^2 + 2(u_{y,x})(\delta u_{y,x}) + (\delta u_{y,x})^2 &= 1 \\
-2\delta u_{x,x} + 2(u_{x,x})(\delta u_{x,x}) + (\delta u_{x,x})^2 + 2(u_{y,x})(\delta u_{y,x}) + (\delta u_{y,x})^2 &= 0
\end{aligned}$$

$$2\delta u_{x,x} \;\; = \;\; 2(u_{x,x})(\delta u_{x,x}) + (\delta u_{x,x})^2 + 2(u_{y,x})(\delta u_{y,x}) + (\delta u_{y,x})^2$$

Neglecting the square of the virtual deformation terms (assuming infinitesimal virtual deformation), and assuming the slender element is much stiffer to axial deformation than to transverse deformation ($u_{x,x} \ll u_{y,x}$),

$$(\delta u_{x,x}(x)) \;\; \approx \;\; (u_{y,x}(x)) \; (\delta u_{y,x}(x)) \tag{16}$$

This specific kind of geometric deformation may be determined from derivitives of shape functions

$$\begin{aligned} u_{y,x}(\boldsymbol{x}, t) &\approx \sum_{n=1}^{N} \psi_{yn,x}(\boldsymbol{x}) \; \bar{u}_n(t) \\ u_{y,x}(\boldsymbol{x}, t) &\approx \boldsymbol{\Psi}_{y,x}(\boldsymbol{x}) \; \bar{\boldsymbol{u}}(t) = \boldsymbol{B}_{\mathrm{g}}(\boldsymbol{x}) \; \delta\bar{\boldsymbol{u}}(t) \end{aligned} \tag{17}$$

and

$$\begin{aligned} \delta u_{y,x}(\boldsymbol{x}, t) &\approx \sum_{n=1}^{N} \psi_{yn,x}(\boldsymbol{x}) \; \delta\bar{u}_n(t) \\ \delta u_{y,x}(\boldsymbol{x}, t) &\approx \boldsymbol{\Psi}_{y,x}(\boldsymbol{x}) \; \delta\bar{\boldsymbol{u}}(t) = \boldsymbol{B}_{\mathrm{g}}(\boldsymbol{x}) \; \delta\bar{\boldsymbol{u}}(t) \end{aligned} \tag{18}$$

Where the terms in $\boldsymbol{B}_{\mathrm{g}}(\boldsymbol{x})$ contain the partial derivitives of the transverse displacement shape functions $\psi_y(\boldsymbol{x})$ with respect to the axial direction coordinate, x.

The accuracy of the approximations (15) and (16) can be quantified in terms of the strains in a displaced bar. Figure 3 shows a bar with four displacement coordinates and Figure 4 shows the errors associated with the finite strain approximation. In this figure, L_1 is the true stretched length of the truss bar, $L_1 = \sqrt{(L_o + u_3 - u_1)^2 + (u_5 - u_2)^2}$, L_2 uses the finite-strain approximation shown above, $L_2 = L_o + (u_3 - u_1) + (1/(2L_o))(u_5 - u_2)^2$, and the logarithmic strain is $\ln(L_1/L_o)$. For a bar stretched to a level of linear strain $(u_3 - u_1)/L_o$ that is significant for most metallic materials, the approximations (15) and (16) are accurate to within 0.001% for rotations $u_{y,x} < 0.1$, at which point the total strain would be approximately 0.005, which is about twice the yield strain for most metals. For analyses of structures incorporating geometric nonlinearity but within the range of elastic behavior of metals, the approximations (15) and (16) for the geometric portion of the deformation are accurate to within one part per million.

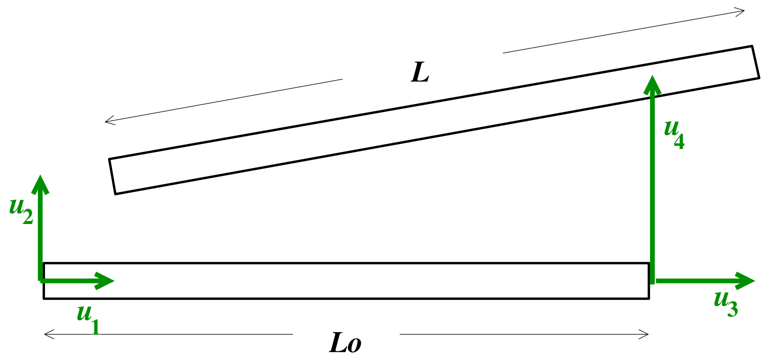

Figure 3. A bar with four displacement coordinates in its original and displaced configurations.

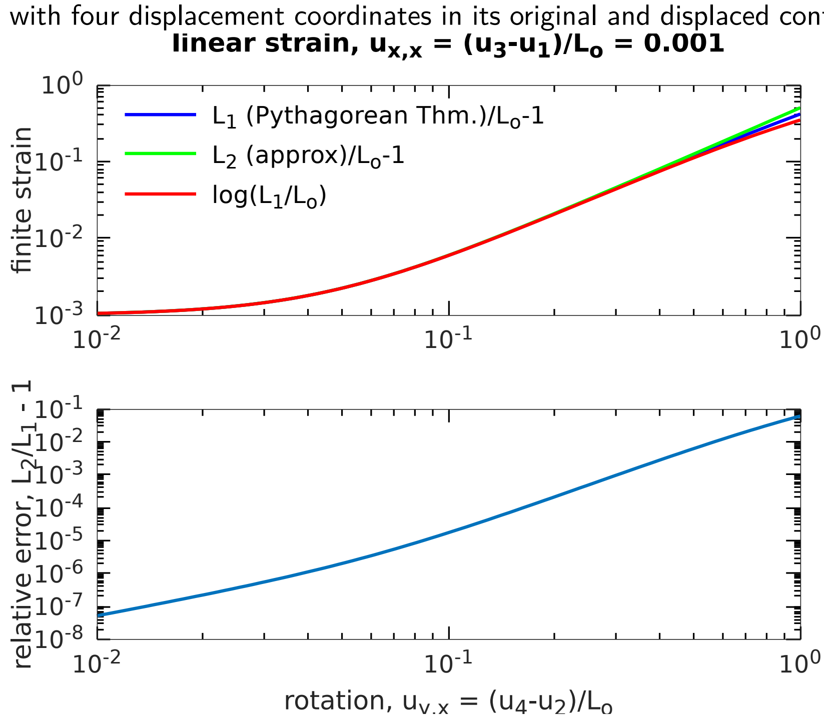

Figure 4. Finite-strain approximations and their associated errors.

1.3 Geometric Deformations in 2D and 3D Solids (Green-Lagrange Strain)

Following the development from the previous section, we can consider the planar displacement of a short line segment of length dl_o to a line segment of length dl. In the original configuration, the line segment has a squared length of

$$dl_o^2 = dx^2 + dy^2$$

and in the displaced configuration it has a squared length of

$$\begin{aligned} dl^2 &= (dx + u_{x,x}dx + u_{x,y}dy)^2 + (dy + u_{y,x}dx + u_{y,y}dy)^2 \\ &= (dx)^2 + (u_{x,x})^2(dx)^2 + (u_{x,y})^2(dy)^2 + 2(u_{x,x})(dx)^2 + 2(u_{x,y})(dx)(dy) + 2(u_{x,x}u_{x,y})(dx)(dy) + \\ &\quad (dy)^2 + (u_{y,x})^2(dx)^2 + (u_{y,y})^2(dy)^2 + 2(u_{y,x})(dx)(dy) + 2(u_{y,y})(dy)^2 + 2(u_{y,x}u_{y,y})(dx)(dy) \end{aligned}$$

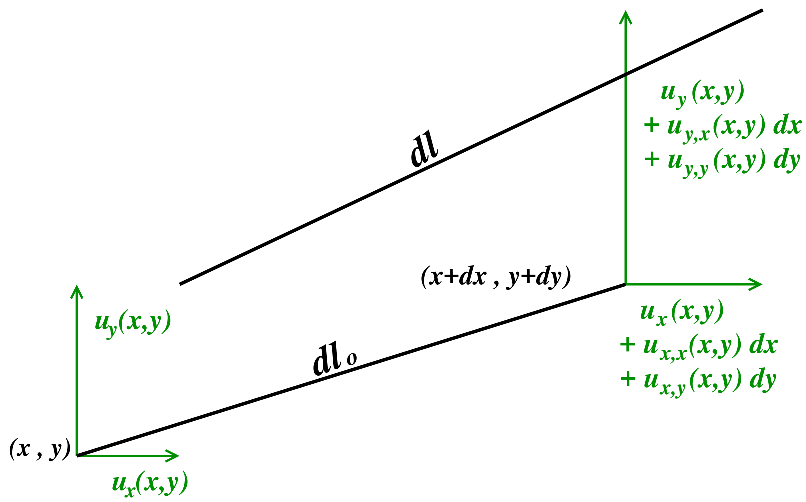

Figure 5. Displacement of line segment dl_o to line segment dl through planar displacements $u_x(x,y)$ and $u_y(x,y)$.

The difference between the squared lengths, $dl^2 - dl_o^2$, is quadratic in dx and dy and can be expressed in a "matrix form."

$$
\begin{aligned}
l^2 - l_o^2 &= 2 \begin{bmatrix} dx \\ dy \end{bmatrix}^{\mathsf{T}} \begin{bmatrix} u_{x,x} + \frac{1}{2}u_{x,x}^2 + \frac{1}{2}u_{y,x}^2 & \frac{1}{2}u_{x,y} + \frac{1}{2}u_{y,x} + \frac{1}{2}u_{x,y}u_{y,x} \\ \frac{1}{2}u_{x,y} + \frac{1}{2}u_{y,x} + \frac{1}{2}u_{x,y}u_{y,x} & u_{y,y} + \frac{1}{2}u_{x,y}^2 + \frac{1}{2}u_{y,y}^2 \end{bmatrix} \begin{bmatrix} dx \\ dy \end{bmatrix} \\
&= 2 \begin{bmatrix} dx \\ dy \end{bmatrix}^{\mathsf{T}} \begin{bmatrix} \epsilon_{xx} & \frac{1}{2}\gamma_{xy} \\ \frac{1}{2}\gamma_{yx} & \epsilon_{yy} \end{bmatrix} \begin{bmatrix} dx \\ dy \end{bmatrix} \qquad (19)
\end{aligned}
$$

This "matrix" is called the *Green-Lagrange strain tensor*, or the *Lagrangian strain tensor*, or the *Green-Saint Venant strain tensor* for plane strain. This relationship may be confirmed in two simple cases:

- $dx = dl_o$, $dy = 0$, $u_{x,x} = \Delta/l_o$, $u_{x,y} = 0$, $u_{y,y} = 0$, $\Rightarrow dl^2 - dl_o^2 = 2l_o\Delta + \Delta^2$.
- $dx = dl_o$, $dy = 0$, $u_{y,x} = \Delta/l_o$, $u_{x,x} = 0$, $u_{y,y} = 0$, $\Rightarrow dl^2 - dl_o^2 = \Delta^2$.

Generalizing this result to three dimensions, the strain-displacement equations for linear strain and geometric deformation are:

$$
\epsilon_{ii} = u_{i,i} + \frac{1}{2}u_{i,i}^2 + \frac{1}{2}u_{j,i}^2 + \frac{1}{2}u_{k,i}^2 = \frac{\partial u_i}{\partial x_i} + \frac{1}{2}\left(\frac{\partial u_i}{\partial x_i}\right)^2 + \frac{1}{2}\left(\frac{\partial u_j}{\partial x_i}\right)^2 + \frac{1}{2}\left(\frac{\partial u_k}{\partial x_i}\right)^2 \qquad (20)
$$

$$
\gamma_{ij} = u_{i,j} + u_{j,i} + u_{i,j}u_{j,j} + u_{j,i}u_{i,i} = \frac{\partial u_i}{\partial x_j} + \frac{\partial u_j}{\partial x_i} + \frac{\partial u_i}{\partial x_j}\frac{\partial u_j}{\partial x_j} + \frac{\partial u_j}{\partial x_i}\frac{\partial u_i}{\partial x_i} \qquad (21)
$$

In the following models, finite deformation effects are limited to $\epsilon_{xx} \approx u_{x,x} + (1/2)u_{y,x}^2$ for the exclusive purpose of deriving geometric stiffness matrices. For metallic materials in which strains are typically around 0.001, this approximation does not compromise accuracy.

1.4 Stress-strain relationship (isotropic elastic solid)

For an isotropic elastic solid with elastic modulus (Young's modulus) E and Poisson's ratio ν, the six strains $\boldsymbol{\epsilon}$ are related to the six stresses $\boldsymbol{\sigma}$ through a material stiffness matrix $\boldsymbol{S}_{\mathrm{e}}$.

$$\left\{ \begin{array}{c} \sigma_{11} \\ \sigma_{22} \\ \sigma_{33} \\ \tau_{12} \\ \tau_{23} \\ \tau_{13} \end{array} \right\} = \frac{E}{(1+\nu)(1-2\nu)} \left[\begin{array}{cccccc} 1-\nu & \nu & \nu & & & \\ \nu & 1-\nu & \nu & & & \\ \nu & \nu & 1-\nu & & & \\ & & & \frac{1}{2}-\nu & & \\ & & & & \frac{1}{2}-\nu & \\ & & & & & \frac{1}{2}-\nu \end{array} \right] \left\{ \begin{array}{c} \epsilon_{11} \\ \epsilon_{22} \\ \epsilon_{33} \\ \gamma_{12} \\ \gamma_{23} \\ \gamma_{13} \end{array} \right\} \quad (22)$$

Stress vector

$$\boldsymbol{\sigma}^{\mathsf{T}}(\boldsymbol{x}, t) \equiv \{ \ \sigma_{11} \ \ \sigma_{22} \ \ \sigma_{33} \ \ \tau_{12} \ \ \tau_{23} \ \ \tau_{13} \ \} \quad (23)$$

$$\boldsymbol{\sigma} = [\ \boldsymbol{S}_{\mathrm{e}}(E, \nu) \ ]_{6\times 6} \ \boldsymbol{\epsilon} \quad (24)$$

1.5 Work of external forces collocated with nodal virtual displacements $\delta\bar{\boldsymbol{u}}$

Quite simply, the set of external forces $\bar{\boldsymbol{f}}$ collocated with nodal virtual displacements $\delta\bar{\boldsymbol{u}}$ is

$$\delta W_{\mathrm{x}} = \bar{\boldsymbol{f}}^{\mathsf{T}}(t) \ \delta\bar{\boldsymbol{u}}(t) \quad (25)$$

1.6 Work of internal inertial forces moving through internal virtual displacements

The inertial force on an accelerating elemental particle of matter of mass $(\rho \, dV)$ is $(\rho \, dV)\ddot{\boldsymbol{u}}(\boldsymbol{x}, t)$ The internal virtual work of these forces moving through collocated virtual displacements throughout an elastic solid is

$$\delta W_{\mathrm{i}} = \int_V \ddot{\boldsymbol{u}}^{\mathsf{T}}(\boldsymbol{x}, t) \ \rho \ \delta\boldsymbol{u}(\boldsymbol{x}, t) \ dV \ ,$$

Substituting the shape function relations (3) and (6),

$$\delta W_{\mathrm{i}} = \int_V \ddot{\bar{\boldsymbol{u}}}^{\mathsf{T}}(t) \boldsymbol{\Psi}^{\mathsf{T}}(\boldsymbol{x}) \ \rho \ \boldsymbol{\Psi}(\boldsymbol{x}) \delta\bar{\boldsymbol{u}}(t) \ dV \ ,$$

and restricting the integrand to position $(\boldsymbol{x})$ dependent factors, leads to

$$\delta W_{\mathrm{i}} = \ddot{\bar{\boldsymbol{u}}}^{\mathsf{T}}(t) \ \int_V \boldsymbol{\Psi}^{\mathsf{T}}(\boldsymbol{x}) \ \rho \ \boldsymbol{\Psi}(\boldsymbol{x}) \ dV \ \delta\bar{\boldsymbol{u}}(t) \ , \quad (26)$$

1.7 Work of internal elastic stresses moving through internal virtual strains

The distribution of internal elastic stresses $\boldsymbol{\sigma}(\boldsymbol{x},t)$ collocated with distributed internal virtual strains $\delta\boldsymbol{\epsilon}(\boldsymbol{x},t)$ is

$$\delta W_{\rm e} = \int_V \boldsymbol{\sigma}^{\sf T}(\boldsymbol{x},t)\ \delta\boldsymbol{\epsilon}(\boldsymbol{x},t)\ dV$$

Substituting the symmetric stress strain relation (22)

$$\delta W_{\rm e} = \int_V \boldsymbol{\epsilon}^{\sf T}(\boldsymbol{x},t)\ \boldsymbol{S}_{\rm e}(E,\nu)\ \delta\boldsymbol{\epsilon}(\boldsymbol{x},t)\ dV\ ,$$

substituting the strain-displacement relation (14)

$$\delta W_{\rm e} = \int_V \bar{\boldsymbol{u}}^{\sf T}(t)\boldsymbol{B}_{\rm e}^{\sf T}(\boldsymbol{x})\ \boldsymbol{S}_{\rm e}(E,\nu)\ \boldsymbol{B}_{\rm e}(\boldsymbol{x})\delta\bar{\boldsymbol{u}}(t)\ dV\ ,$$

and restricting the integrand to position ($\boldsymbol{x}$) dependent factors, leads to

$$\delta W_{\rm e} = \bar{\boldsymbol{u}}^{\sf T}(t)\ \int_V \boldsymbol{B}_{\rm e}^{\sf T}(\boldsymbol{x})\ \boldsymbol{S}_{\rm e}(E,\nu)\ \boldsymbol{B}_{\rm e}(\boldsymbol{x})\ dV\ \delta\bar{\boldsymbol{u}}(t)\ , \tag{27}$$

1.8 Work of internal axial forces moving through internal virtual geometric displacements

In a slender prismatic solid loaded axially and displacing laterally, the work of an axial forces $N(x)$, moving through the axial virtual displacements arising from transverse displacements (16) is

$$\delta W_{\rm g} = \int_0^L N(x)\ (u_{y,x}(x))\ (\delta u_{y,x}(x))\ dx$$

Substituting the shape function relations (17) and (18) for $u_{y,x}$,

$$\delta W_{\rm g} = \int_0^L N(x)\ \bar{\boldsymbol{u}}^{\sf T}(t)\boldsymbol{B}_{\rm g}^{\sf T}(\boldsymbol{x})\ \boldsymbol{B}_{\rm g}(\boldsymbol{x})\delta\bar{\boldsymbol{u}}(t)\ dx$$

and restricting the integrand to position ($\boldsymbol{x}$) dependent factors, leads to

$$\delta W_{\rm g} = \bar{\boldsymbol{u}}^{\sf T}(t)\ \int_0^L N(x)\ \boldsymbol{B}_{\rm g}^{\sf T}(\boldsymbol{x})\ \boldsymbol{B}_{\rm g}(\boldsymbol{x})\ dx\ \delta\bar{\boldsymbol{u}}(t) \tag{28}$$

1.9 Equating internal virtual work to external virtual work

Using (25), (26), (27), and (28) to equate internal virtual work to external virtual work,

$$\begin{aligned} \delta W_{\rm i} + \delta W_{\rm e} + \delta W_{\rm g} &= \delta W_{\rm x} \qquad (29) \\ \ddot{\bar{\boldsymbol{u}}}^{\sf T}(t)\ \int_V \boldsymbol{\Psi}^{\sf T}(\boldsymbol{x})\ \rho\ \boldsymbol{\Psi}(\boldsymbol{x})\ dV\ \delta\bar{\boldsymbol{u}}(t) &+ \\ \bar{\boldsymbol{u}}^{\sf T}(t)\ \int_V \boldsymbol{B}_{\rm e}^{\sf T}(\boldsymbol{x})\ \boldsymbol{S}_{\rm e}(E,\nu)\ \boldsymbol{B}_{\rm e}(\boldsymbol{x})\ dV\ \delta\bar{\boldsymbol{u}}(t) &+ \\ \bar{\boldsymbol{u}}^{\sf T}(t)\ \int_0^L N(x)\ \boldsymbol{B}_{\rm g}^{\sf T}(\boldsymbol{x})\ \boldsymbol{B}_{\rm g}(\boldsymbol{x})\ dx\ \delta\bar{\boldsymbol{u}}(t) &= \bar{\boldsymbol{f}}^{\sf T}(t)\ \delta\bar{\boldsymbol{u}}(t) \end{aligned}$$

Since admissible displacement variations must be independent and arbitrary, we may factor out the $\delta\bar{\boldsymbol{u}}(t)$ from each term. So doing, and taking the transpose of both sides,

$$\begin{aligned} \left[\int_V \boldsymbol{\Psi}^{\mathsf{T}}(\boldsymbol{x}) \ \rho \ \boldsymbol{\Psi}(\boldsymbol{x}) \ dV \right] \ddot{\bar{\boldsymbol{u}}}(t) & \ + \\ \left[\int_V \boldsymbol{B}_{\mathrm{e}}^{\mathsf{T}}(\boldsymbol{x}) \ \boldsymbol{S}_{\mathrm{e}}(E,\nu) \ \boldsymbol{B}_{\mathrm{e}}(\boldsymbol{x}) \ dV \right] \bar{\boldsymbol{u}}(t) & \ + \\ \left[\int_0^L N(x) \ \boldsymbol{B}_{\mathrm{g}}^{\mathsf{T}}(\boldsymbol{x}) \ \boldsymbol{B}_{\mathrm{g}}(\boldsymbol{x}) \ dx \right] \bar{\boldsymbol{u}}(t) & \ = \ \bar{\boldsymbol{f}}(t) \end{aligned}$$

in which the matrix in the first term is a mass matrix, the matrix in the second term is an elastic stiffness matrix, and the matrix in the third term is the geometric stiffness matrix.

$$\boldsymbol{M} \ \ddot{\bar{\boldsymbol{u}}}(t) + \boldsymbol{K}_{\mathrm{e}} \ \bar{\boldsymbol{u}}(t) + \boldsymbol{K}_{\mathrm{g}}(\bar{\boldsymbol{u}}) \ \bar{\boldsymbol{u}}(t) = \boldsymbol{f}(t)$$

where

$$\boldsymbol{M} = \int_V \boldsymbol{\Psi}^{\mathsf{T}}(\boldsymbol{x}) \ \rho \ \boldsymbol{\Psi}(\boldsymbol{x}) \ dV \qquad (30)$$

$$\boldsymbol{K}_{\mathrm{e}} = \int_V \boldsymbol{B}_{\mathrm{e}}^{\mathsf{T}}(\boldsymbol{x}) \ \boldsymbol{S}_{\mathrm{e}}(E,\nu) \ \boldsymbol{B}_{\mathrm{e}}(\boldsymbol{x}) \ dV \qquad (31)$$

$$\boldsymbol{K}_{\mathrm{g}}(\bar{\boldsymbol{u}}) = \int_0^L N(x) \ \boldsymbol{B}_{\mathrm{g}}^{\mathsf{T}}(\boldsymbol{x}) \ \boldsymbol{B}_{\mathrm{g}}(\boldsymbol{x}) \ dx \qquad (32)$$

The topic of structural damping element matrices is introduced in section 7.

2 Bar Element Matrices

2D prismatic homogeneous isotropic truss bar.

Uniform uni-axial stress	$\boldsymbol{\sigma}^{\mathsf{T}} = \{\sigma_{xx}, 0, 0, 0, 0, 0\}^{\mathsf{T}}$
Corresponding strain	$\boldsymbol{\epsilon}^{\mathsf{T}} = (\sigma_{xx}/E)\,\{1, -\nu, -\nu, 0, 0, 0\}^{\mathsf{T}}$.
Incremental strain energy	$dU = \frac{1}{2}\boldsymbol{\sigma}^{\mathsf{T}}\boldsymbol{\epsilon}\; dV = \frac{1}{2}\sigma_{xx}\epsilon_{xx}\; dV = \frac{1}{2}E\epsilon_{xx}^2\; dV$

2.1 Bar Displacements

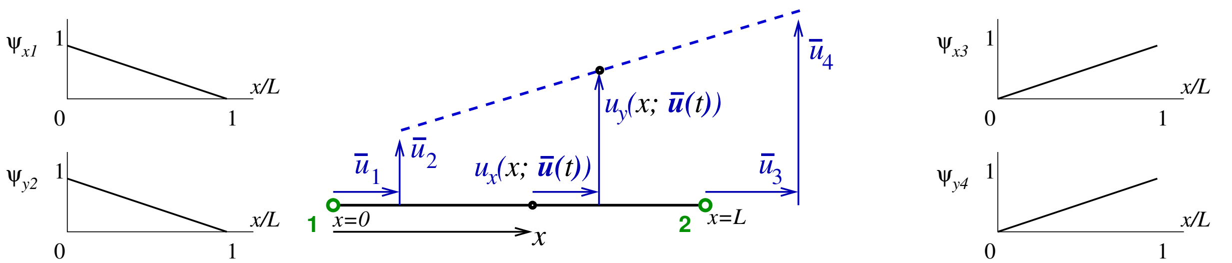

Figure 6. Truss bar element coordinates, shape functions, and displacements.

Internal displacements *along* the bar in terms of $\bar{u}_1(t)$ and $\bar{u}_3(t)$

$$u_x(x,t) = \left(1 - \frac{x}{L}\right)\bar{u}_1(t) + \left(\frac{x}{L}\right)\bar{u}_3(t) \tag{33}$$

$$= \psi_{x1}(x)\;\bar{u}_1(t) + \psi_{x3}(x)\;\bar{u}_3(t) \tag{34}$$

Internal displacements *across* the bar in terms of $\bar{u}_2(t)$ and $\bar{u}_4(t)$

$$u_y(x,t) = \left(1 - \frac{x}{L}\right)\bar{u}_2(t) + \left(\frac{x}{L}\right)\bar{u}_4(t) \tag{35}$$

$$= \psi_{y2}(x)\;\bar{u}_2(t) + \psi_{y4}(x)\;\bar{u}_4(t) \tag{36}$$

Shape function matrix

$$\boldsymbol{\Psi}(x) = \left[\begin{array}{c|c|c|c} 1 - x/L & 0 & x/L & 0 \\ \hline 0 & 1 - x/L & 0 & x/L \end{array}\right] \tag{37}$$

Shape function matrix equation for $u_x(x,t)$ and $u_y(x,t)$ in terms of $\boldsymbol{\Psi}(x)$ and $\bar{\boldsymbol{u}}(t)$.

$$\left[\begin{array}{c} u_x(x,t) \\ u_y(x,t) \end{array}\right] = \boldsymbol{\Psi}(x)\;\bar{\boldsymbol{u}}(t) \tag{38}$$

2.2 Bar Mass Matrix

$$\bar{\boldsymbol{M}} = \int_{x=0}^{L} \left[\boldsymbol{\Psi}^{\mathsf{T}}(x) \; \rho \; \boldsymbol{\Psi}(x) \right] \; A \; dx \tag{39}$$

$$= \rho A \int_{x=0}^{L} \begin{bmatrix} (1-\frac{x}{L})^2 & 0 & (1-\frac{x}{L})(\frac{x}{L}) & 0 \\ 0 & (1-\frac{x}{L})^2 & 0 & (1-\frac{x}{L})(\frac{x}{L}) \\ (\frac{x}{L})(1-\frac{x}{L}) & 0 & (\frac{x}{L})^2 & 0 \\ 0 & (\frac{x}{L})(1-\frac{x}{L}) & 0 & (\frac{x}{L})^2 \end{bmatrix} dx \tag{40}$$

$$= \frac{1}{6}\rho A L \begin{bmatrix} 2 & 0 & 1 & 0 \\ 0 & 2 & 0 & 1 \\ 1 & 0 & 2 & 0 \\ 0 & 1 & 0 & 2 \end{bmatrix} \tag{41}$$

2.3 Bar Elastic Stiffness Matrix

Strain-displacement relation for elastic stiffness

$$\epsilon_{xx} = \frac{\partial u_x}{\partial x} \tag{42}$$

$$= \psi_{x1,x}\bar{u}_1 + \psi_{x3,x}\bar{u}_3 \tag{43}$$

$$= \left(-\frac{1}{L}\right)\bar{u}_1 + \left(\frac{1}{L}\right)\bar{u}_3 \tag{44}$$

$$= \left[-\frac{1}{L} \;\; 0 \;\; \frac{1}{L} \;\; 0 \right] \bar{\boldsymbol{u}} \tag{45}$$

$$= \boldsymbol{B}_{\mathrm{e}} \; \bar{\boldsymbol{u}} \tag{46}$$

$$\boldsymbol{B}_{\mathrm{e}} = \left[-\frac{1}{L} \;\; 0 \;\; \frac{1}{L} \;\; 0 \right]. \tag{47}$$

Elastic stiffness

$$\bar{\boldsymbol{K}}_{\mathrm{e}} = \int_{x=0}^{L} \left[\boldsymbol{B}_{\mathrm{e}}^{\mathsf{T}} \; E \; \boldsymbol{B}_{\mathrm{e}} \right] \; A \; dx \tag{48}$$

$$= EA \int_{x=0}^{L} \begin{bmatrix} 1/L^2 & 0 & -1/L^2 & 0 \\ 0 & 0 & 0 & 0 \\ -1/L^2 & 0 & 1/L^2 & 0 \\ 0 & 0 & 0 & 0 \end{bmatrix} dx \tag{49}$$

$$= \frac{EA}{L} \begin{bmatrix} 1 & 0 & -1 & 0 \\ 0 & 0 & 0 & 0 \\ -1 & 0 & 1 & 0 \\ 0 & 0 & 0 & 0 \end{bmatrix} \tag{50}$$

2.4 Bar Geometric Stiffness Matrix

Strain-displacement relation for geometric stiffness

$$
\begin{aligned}
u_{y,x} &= \frac{\partial u_y}{\partial x} && (51)\\
&= \psi_{y2,x}\bar{u}_2 + \psi_{y4,x}\bar{u}_4 && (52)\\
&= \left(-\frac{1}{L}\right)\bar{u}_2 + \left(\frac{1}{L}\right)\bar{u}_4 && (53)\\
&= \boldsymbol{B}_\mathrm{g}\ \bar{\boldsymbol{u}} && (54)\\
\boldsymbol{B}_\mathrm{g} &= \begin{bmatrix} 0 & -\frac{1}{L} & 0 & \frac{1}{L} \end{bmatrix}. && (55)
\end{aligned}
$$

Geometric Stiffness

$$
\begin{aligned}
\bar{\boldsymbol{K}}_\mathrm{g} &= \int_{x=0}^{L} \left[N(x)\ \boldsymbol{B}_\mathrm{g}^\mathsf{T}\ \boldsymbol{B}_\mathrm{g} \right]\ dx && (56)\\
N(x) &= \frac{EA}{L}(\bar{u}_3 - \bar{u}_1) && (57)\\
\bar{\boldsymbol{K}}_\mathrm{g}(\bar{\boldsymbol{u}}) &= \frac{EA}{L}(\bar{u}_3 - \bar{u}_1)\int_{x=0}^{L} \begin{bmatrix} 0 & 0 & 0 & 0 \\ 0 & 1/L^2 & 0 & -1/L^2 \\ 0 & 0 & 0 & 0 \\ 0 & -1/L^2 & 0 & 1/L^2 \end{bmatrix} dx && (58)\\
&= \frac{EA}{L^2}(\bar{u}_3 - \bar{u}_1) \begin{bmatrix} 0 & 0 & 0 & 0 \\ 0 & 1 & 0 & -1 \\ 0 & 0 & 0 & 0 \\ 0 & -1 & 0 & 1 \end{bmatrix} && (59)
\end{aligned}
$$

3 Bernoulli-Euler Beam Element Matrices

Assumptions:
2D prismatic homogeneous isotropic beam element (E, I, A are constant);
neglect shear deformation (γ_{xy} is negligible);
neglect rotatory inertia ($u_{y,xtt}$ is negligible);
Plane sections normal to the neutral axis remain plane and normal to the neutral axis. ($\epsilon_{xx} = u_{x,x} - u_{y,xx}y$, $M = EIu_{y,xx}$);
No distributed load along the beam, (shear is constant).

3.1 Bernoulli-Euler Beam Coordinates and Internal Displacements

Consider the geometry of a deformed beam. The functions $u_x(x)$ and $u_y(x)$ describe the translation of the beam's neutral axis, in the x and y directions.

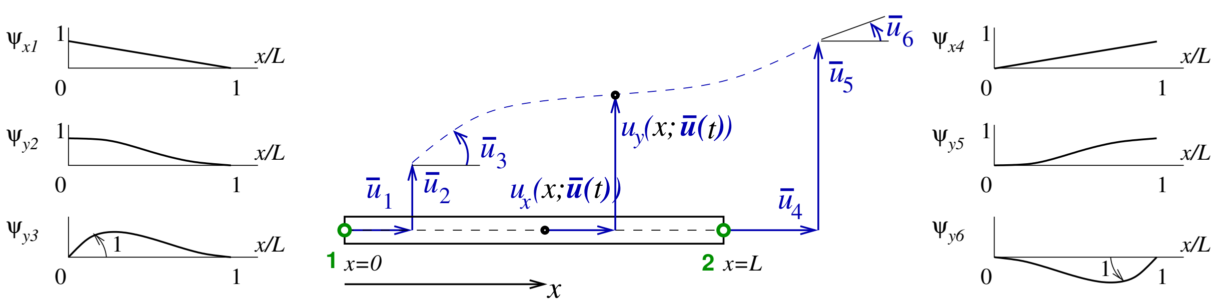

Figure 7. Bernoulli-Euler beam element coordinates, shape functions, and displacements.

The internal displacements of the neutral axis $u_x(x,t)$ and $u_y(x,t)$ are expressed in terms of a set of shape functions, $\psi_{xn}(x)$ and $\psi_{yn}(x)$, and the end displacements $(\bar{u}_1(t), \bar{u}_2(t), \bar{u}_4(t), \bar{u}_5(t))$ and the end rotations $(\bar{u}_3(t), \bar{u}_6(t))$.

$$
\begin{aligned}
u_x(x,t) &= \sum_{n=1}^{6} \psi_{xn}(x)\ \bar{u}_n(t) \\
u_y(x,t) &= \sum_{n=1}^{6} \psi_{yn}(x)\ \bar{u}_n(t)
\end{aligned}
$$

The shape functions $\psi_{xn}(x)$ and $\psi_{yn}(x)$ satisfy the the differential equation describing *static* bending of a Bernoulli-Euler beam ($M(x) = EI\psi_y''(x)$) with a specified unit displacement at each nodal coordinate, produced by forces collocated with the six element coordinates. With this kind of loading, internal bending moments $M(x)$ vary linearly along the neutral axis and the transverse displacements of the neutral axis are cubic polynomials. The Bernoulli-Euler beam model neglects the effects of shear deformation and rotatory inertia. For bending of the neutral axis,

$$
\begin{aligned}
\psi_{y2}(x) &= 1-3\left(\frac{x}{L}\right)^2+2\left(\frac{x}{L}\right)^3 \\
\psi_{y3}(x) &= \left(\frac{x}{L}-2\left(\frac{x}{L}\right)^2+\left(\frac{x}{L}\right)^3\right)L \\
\psi_{y5}(x) &= 3\left(\frac{x}{L}\right)^2-2\left(\frac{x}{L}\right)^3 \\
\psi_{y6}(x) &= \left(-\left(\frac{x}{L}\right)^2+\left(\frac{x}{L}\right)^3\right)L
\end{aligned}
$$

and $\psi_{y1}=\psi_{y4}=0$. The extension of the neutral axis uses the same shape functions as the model for a bar described in the previous section.

$$
\begin{aligned}
\psi_{x1}(x) &= 1-\frac{x}{L} \\
\psi_{x4}(x) &= \frac{x}{L}
\end{aligned}
$$

and $\psi_{x2}=\psi_{x3}=\psi_{x5}=\psi_{x6}=0$. The shape function matrix is

$$
\boldsymbol{\Psi}(x)=\left[\begin{array}{c|c|c|c|c|c}
1-\frac{x}{L} & 0 & 0 & \frac{x}{L} & 0 & 0 \\
\hline
0 & 1-3\left(\frac{x}{L}\right)^2+2\left(\frac{x}{L}\right)^3 & \left(\frac{x}{L}-2\left(\frac{x}{L}\right)^2+\left(\frac{x}{L}\right)^3\right)L & 0 & 3\left(\frac{x}{L}\right)^2-2\left(\frac{x}{L}\right)^3 & \left(-\left(\frac{x}{L}\right)^2+\left(\frac{x}{L}\right)^3\right)L
\end{array}\right] \tag{60}
$$

and relates the neutral axis displacements to the displacements of the six beam element coordinates.

$$
\left[\begin{array}{c} u_x(x,t) \\ u_y(x,t) \end{array}\right] = \boldsymbol{\Psi}(x)\ \bar{\boldsymbol{u}}(t) \tag{61}
$$

3.2 Bernoulli-Euler Beam Mass Matrix

With the shape functions above, the mass matrix is a direct application of equation (30).

$$
\bar{\boldsymbol{M}} \;=\; \int_{x=0}^{L} \left[\boldsymbol{\Psi}^{\mathsf{T}}(x)\ \rho\ \boldsymbol{\Psi}(x)\right]_{6\times 6}\ A\ dx \tag{62}
$$

3.3 Bernoulli-Euler Beam Elastic Stiffness Matrix

Strain-displacement relations for elastic stiffens

The strain normal to the cross section, ϵ_{xx}, within a beam is the strain of pure extension $(\partial u_x/\partial x)$, plus the bending strain, $-(\partial^2 u_y/\partial x^2)y$.

$$
\begin{aligned}
\epsilon_{xx} &= \frac{\partial u_x}{\partial x}-\frac{\partial^2 u_y}{\partial x^2}\ y = u_{x,x}-u_{y,xx}\ y \\
&= \sum_{n=1}^{6}\frac{\partial}{\partial x}\psi_{xn}(x)\ \bar{u}_n-\sum_{n=1}^{6}\frac{\partial^2}{\partial x^2}\psi_{yn}(x)\ y\ \bar{u}_n=\sum_{n=1}^{6}\psi_{xn,x}(x)\ \bar{u}_n-\sum_{n=1}^{6}\psi_{yn,xx}(x)\ y\ \bar{u}_n \\
&= \sum_{n=1}^{6} B_{\mathrm{e}n}(x,y)\ \bar{u}_n \\
&= \boldsymbol{B}_{\mathrm{e}}(x,y)\ \bar{\boldsymbol{u}}
\end{aligned} \tag{63}
$$

where

$$\boldsymbol{B}_{\mathrm{e}}(x,y) = \left[-\frac{1}{L},\ \ \frac{6y}{L^2} - \frac{12xy}{L^3},\ \ \frac{4y}{L} - \frac{6xy}{L^2},\ \ \frac{1}{L},\ \ \frac{-6y}{L^2} + \frac{12xy}{L^3},\ \ \frac{2y}{L} - \frac{6xy}{L^2} \right] . \tag{64}$$

Elastic Stiffness Matrix

The elastic stiffness matrix can be found from directly from equation (31) by including only axial strains ϵ_{xx} and the elastic modulus E.

$$\bar{\boldsymbol{K}}_{\mathrm{e}} \ = \ \int_{x=0}^{L} \int_A \left[\boldsymbol{B}_{\mathrm{e}}^{\mathsf{T}}(x,y)\ E\ \boldsymbol{B}_{\mathrm{e}}(x,y) \right]_{6\times 6}\ dA\ dx. \tag{65}$$

Note that this integral involves terms such as $\int_A y^2 dA$ and $\int_A y dA$ in which the origin of the coordinate axis is placed at the centroid of the section. The integral $\int_A y^2 dA$ is the bending moment of inertia for the cross section, I, and the integral $\int_A y dA$ is zero.

3.4 Bernoulli-Euler Beam Geometric Stiffness Matrix

Strain-displacement relation for geometric stiffness

$$\begin{aligned}
u_{y,x} &= \frac{\partial u_y}{\partial x} && (66)\\
&= \psi_{y2,x}\bar{u}_2 + \psi_{y3,x}\bar{u}_3 + \psi_{y5,x}\bar{u}_5 + \psi_{y6,x}\bar{u}_6 && (67)\\
&= \left(-6x/L^2 + 6x^2/L^3\right)\ \bar{u}_2 + \left(1/L - 4x/L^2 + 3x^2/L^3\right) L\ \bar{u}_3 + \\
&\quad \left(6x/L^2 - 6x^2/L^3\right)\ \bar{u}_5 + \left(-2x/L^2 + 3x^2/L^3\right) L\ \bar{u}_6 && (68)\\
&= \sum_{n=1}^{6} \boldsymbol{B}_{\mathrm{g}n}\ \bar{u}_n && (69)\\
&= \boldsymbol{B}_{\mathrm{g}}\ \bar{\boldsymbol{u}} && (70)
\end{aligned}$$

$$\boldsymbol{B}_{\mathrm{g}} = \left[\ 0\ ,\ \left(-6x/L^2 + 6x^2/L^3\right)\ ,\ \left(1/L - 4x/L^2 + 3x^2/L^3\right) L\ ,\ 0\ ,\ \left(6x/L^2 - 6x^2/L^3\right)\ ,\ \left(-2x/L^2 + 3x^2/L^3\right) L\ \right] \tag{71}$$

Geometric Stiffness

In a beam element without internal loads, the internal axial force $N(x)$ is constant along its length, $N(x) = (EA/L)(\bar{u}_4 - \bar{u}_1)$, and the geometric stiffness matrix is a direct application of equation (32).

$$\bar{\boldsymbol{K}}_{\mathrm{g}}(\bar{\boldsymbol{u}}) \ = \ \frac{EA}{L}(\bar{u}_4 - \bar{u}_1) \int_{x=0}^{L} \left[\ \boldsymbol{B}_{\mathrm{g}}^{\mathsf{T}}(x)\ \boldsymbol{B}_{\mathrm{g}}(x) \right]\ dx \tag{72}$$

The mass, elastic stiffness, and geometric stiffness matrices involve integrals of symmetric matrices, $[\boldsymbol{\Psi}^{\mathsf{T}}(x)\boldsymbol{\Psi}(x)]$, $[\boldsymbol{B}_{\mathrm{e}}^{\mathsf{T}}(x,y)\boldsymbol{B}_{\mathrm{e}}(x,y)]$, and $[\boldsymbol{B}_{\mathrm{g}}^{\mathsf{T}}(x)\boldsymbol{B}_{\mathrm{g}}(x)]$. This laborious and delicate task may be carried out using symbolic math software, as shown in the next section.

3.5 Bernoulli-Euler Beam matrix integrals in Maple

```
# Shape Function matrix ... 2 by 6 ...
> P := < (1-x/L) , 0 , 0 , x/L , 0 , 0 ; \
       0 , 1-3*(x/L)^2 + 2*(x/L)^3 , (x/L - 2*(x/L)^2 + (x/L)^3)*L , 0 , 3*(x/L)^2-2*(x/L)^3 , (-(x/L)^2+(x/L)^3)*L >;

# Strain-Displacement Relation for elastic stiffness ... 1 by 6 ...
> Be := < -1/L, 6*y/L^2 - 12*x*y/L^3 , 4*y/L - 6*x*y/L^2 , 1/L , -6*y/L^2+12*x*y/L^3 , 2*y/L - 6*x*y/L^2 >^+;

# Strain-Displacement Relation for geometric stiffness ... 1 by 6 ...
> Bg := < 0 , (-6*x/L^2 + 6*x^2/L^3) , (1/L-4*x/L^2+3*x^2/L^3)*L , 0 , (6*x/L^2-6*x^2/L^3) , (-2*x/L^2+3*x^2/L^3)*L >^+;

# Mass Matrix ... (not shown here)
> M := map ( int, pA*(P^+ . P ) , x=0..L );

# Elastic Stiffness Matrix ... just the integral along the x-axis ... needs manual editing ...

> KedA := map ( int , E * Be^+ . Be , x=0..L );

           [                         E y                              E y    ]
           [ E/L          0        - ---      - E/L         0         ---    ]
           [                           L                                L    ]
           [                                                                 ]
           [                 2           2                      2          2 ]
           [          12 E y       6 E y                 12 E y      6 E y   ]
           [  0       -------      ------        0      - -------    ------ ]
           [              3            2                     3           2   ]
           [             L            L                     L           L    ]
           [                                                                 ]
           [                2            2                     2           2 ]
           [  E y     6 E y        4 E y       E y       6 E y       2 E y   ]
           [- ---     ------       ------      ---      - ------      ------ ]
           [   L          2           L          L           2          L    ]
           [             L                                  L                ]
   KedA := [                                                                 ]
           [                        E y                                E y   ]
           [- E/L         0         ---        E/L          0        - ---   ]
           [                          L                                  L   ]
           [                                                                 ]
           [                  2           2                    2            2]
           [           12 E y       6 E y               12 E y       6 E y ]
           [  0      - -------    - ------       0      -------     - ------]
           [               3            2                  3             2  ]
           [              L            L                  L             L   ]
           [                                                                 ]
           [                2            2                     2           2 ]
           [ E y      6 E y        2 E y        E y      6 E y       4 E y   ]
           [ ---      ------       ------     - ---     - ------      ------ ]
           [  L           2           L           L          2          L    ]
           [             L                                  L                ]

# to manually carry out the integral over the cross section area,
# * multiply all terms without a "y" by "A" ... the integral of dA is A
# * set all terms with just "y" equal to 0 ... the origin is at the centroid so the integral of y dA is zero
# * change all "y^2" to "I" ... the integral of y^2 dA equals I

# Geometric Stiffness Matrix ... (not shown here)
> Kg := map ( int, NL*(Bg^+ . Bg ) , x=0..L );
```

3.6 Bernoulli-Euler Beam Element Mass and Stiffness Matrices

Substituting the expressions for the shape functions $\boldsymbol{\Psi}(x)$ and the strain-displacement relations $\boldsymbol{B}_{\rm e}$ and $\boldsymbol{B}_{\rm g}$ into the formulations for element stiffness matrices, (62), (65), and (72), results in element mass and stiffness matrices $\bar{\boldsymbol{M}}$, $\bar{\boldsymbol{K}}_{\rm e}$, and $\bar{\boldsymbol{K}}_{\rm g}$.

$$\bar{\boldsymbol{M}} = \frac{\rho A L}{420} \begin{bmatrix} 140 & 0 & 0 & 70 & 0 & 0 \\ 0 & 156 & 22L & 0 & 54 & -13L \\ 0 & 22L & 4L^2 & 0 & 13L & -3L^2 \\ 70 & 0 & 0 & 140 & 0 & 0 \\ 0 & 54 & 13L & 0 & 156 & -22L \\ 0 & -13L & -3L^2 & 0 & -22L & 4L^2 \end{bmatrix} \tag{73}$$

$$\bar{\boldsymbol{K}}_{\rm e} = \begin{bmatrix} \frac{EA}{L} & 0 & 0 & -\frac{EA}{L} & 0 & 0 \\ 0 & \frac{12EI}{L^3} & \frac{6EI}{L^2} & 0 & -\frac{12EI}{L^3} & \frac{6EI}{L^2} \\ 0 & \frac{6EI}{L^2} & \frac{4EI}{L} & 0 & -\frac{6EI}{L^2} & \frac{2EI}{L} \\ -\frac{EA}{L} & 0 & 0 & \frac{EA}{L} & 0 & 0 \\ 0 & -\frac{12EI}{L^3} & -\frac{6EI}{L^2} & 0 & \frac{12EI}{L^3} & -\frac{6EI}{L^2} \\ 0 & \frac{6EI}{L^2} & \frac{2EI}{L} & 0 & -\frac{6EI}{L^2} & \frac{4EI}{L} \end{bmatrix} \tag{74}$$

$$\bar{\boldsymbol{K}}_{\rm g}(\bar{\boldsymbol{u}}) = \frac{EA}{L^2}(\bar{u}_4 - \bar{u}_1) \begin{bmatrix} 0 & 0 & 0 & 0 & 0 & 0 \\ 0 & \frac{6}{5} & \frac{L}{10} & 0 & -\frac{6}{5} & \frac{L}{10} \\ 0 & \frac{L}{10} & \frac{2L^2}{15} & 0 & -\frac{L}{10} & -\frac{L^2}{30} \\ 0 & 0 & 0 & 0 & 0 & 0 \\ 0 & -\frac{6}{5} & -\frac{L}{10} & 0 & \frac{6}{5} & -\frac{L}{10} \\ 0 & \frac{L}{10} & -\frac{L^2}{30} & 0 & -\frac{L}{10} & \frac{2L^2}{15} \end{bmatrix} \tag{75}$$

4 Timoshenko Beam Element Matrices

2D prismatic homogeneous isotropic beam element, including shear deformation and rotatory inertia

Consider again the geometry of a deformed beam. When shear deformations are included sections that are originally perpendicular to the neutral axis may not be perpendicular to the neutral axis after deformation.

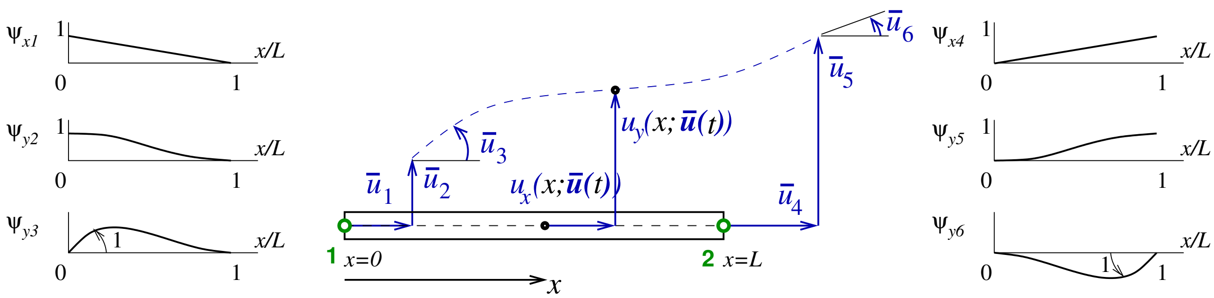

Figure 8. Timoshenko beam element coordinates, shape functions, and displacements.

The functions $u_x(x)$ and $u_y(x)$ describe the translation of the beam's neutral axis, in the x and y directions. If the beam is not slender (length/depth < 5), then shear strains can contribute significantly to the strain energy within the beam. The deformed shape of slender beams is different from the deformed shape of stocky beams. In general, beams carry a bending moment $M(x)$ and shear forces $S(x)$ The moment is related to transverse bending displacements $u_{(\mathrm{b})}(x)$ and axial strain ϵ_{xx}. The shear force is related to transverse shear displacements $u_{(\mathrm{s})}(x)$ and shear strain γ_{xy}. So the strain energy has a bending component and a shearing component.

$$
\begin{aligned}
U &= \frac{1}{2}\int_V \boldsymbol{\sigma}^{\mathsf{T}}\boldsymbol{\epsilon}\; dV \\
&= \frac{1}{2}\int_V \sigma_{xx}\epsilon_{xx}\; dV + \frac{1}{2}\int_V \tau_{xy}\gamma_{xy}\; dV \\
&= \frac{1}{2}\int_0^L \int_A \frac{M(x)y}{I}\frac{M(x)y}{EI}\; dA\; dx + \frac{1}{2}\int_0^L \int_A \frac{SQ(y)}{Ib(y)}\frac{SQ(y)}{GIb(y)}\; dA\; dx \\
&= \frac{1}{2}\int_0^L \frac{M(x)^2}{EI^2}\int_A y^2\; dA\; dx + \frac{1}{2}\int_0^L \frac{S^2}{GI^2}\int_A \frac{Q(y)^2}{b(y)^2}\; dA\; dx \\
&= \frac{1}{2}\int_0^L \frac{M(x)^2}{EI}\; dx + \frac{1}{2}\int_0^L \frac{S^2}{G(A/\alpha)}\; dx
\end{aligned}
\tag{76}
$$

where the *shear area coefficient* α reduces the cross section area to account for the non-uniform distribution of shear stresses in the cross section,

$$\alpha = \frac{A}{I^2}\int_A \frac{Q(y)^2}{b(y)^2}\; dA\;.$$

For solid rectangular sections $\alpha = 6/5$ and for solid circular sections $\alpha = 10/9$ [2, 3, 4, 5, 8].

4.1 Timoshenko Beam Coordinates and Internal Displacements (including shear deformation effects)

The transverse deformation of a beam with shear and bending strains may be separated into a portion related to bending deformation and a portion related to shear deformation,

$$u_y(x,t) = u_{(\mathrm{b})y}(x) + u_{(\mathrm{s})y}(x) \tag{77}$$

The bending and shear deformations are related to bending moments and shear forces, respectively.

$$EI u''_{(\mathrm{b})y}(x) = M(x) = -M_1\left(1 - \frac{x}{L}\right) + M_2\left(\frac{x}{L}\right) \tag{78}$$

$$G(A/\alpha) u'_{(\mathrm{s})y}(x) = S(x) = -\frac{1}{L}(M_1 + M_2) \tag{79}$$

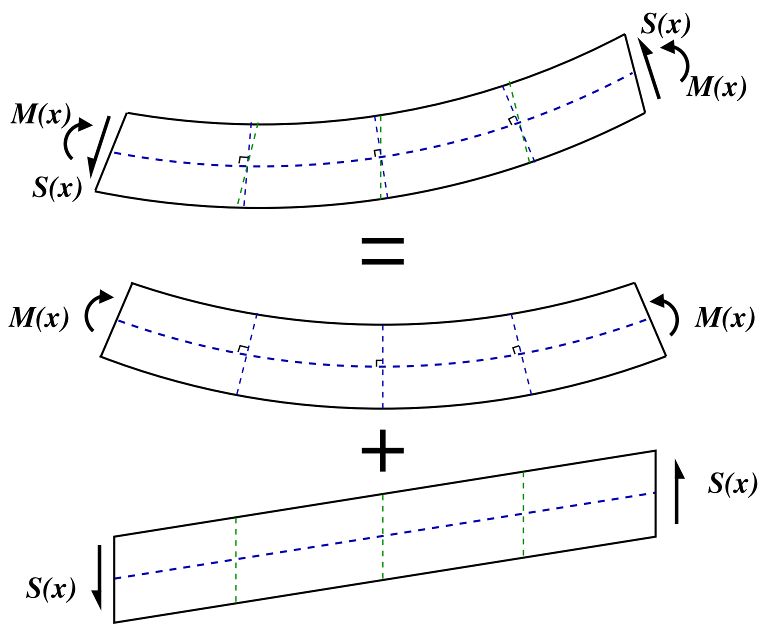

Figure 9. Rotations of cross sections in a Timoshenko beam element, blue: bending $u'_{(\mathrm{b})}(x)$ and green: shear $u'_{(\mathrm{s})}(x)$

Within a beam element (loaded at its end nodes), the shear force is constant and the bending moment varies linearly from M_1 at node 1 to M_2 at node 2. Since the bending moment is (approximately) proportional to $u''_{(\mathrm{b})y}(x)$, the bending deflections within the element must be cubic in x. Similarly, since the shear force is proportional to $u'_{(\mathrm{s})y}(x)$, the shear deflections within the element must be linear in x. These functions may be postulated as

$$u_{(\mathrm{b})y}(x) = c_0 + c_1\left(\frac{x}{L}\right) + c_2\left(\frac{x}{L}\right)^2 + c_3\left(\frac{x}{L}\right)^3 \tag{80}$$

$$u_{(\mathrm{s})y}(x) = d_0 + d_1\left(\frac{x}{L}\right) \tag{81}$$

where each coefficient c_i and d_i has units of deflection (length). In the superimposed solution $u_y(x) = u_{(\mathrm{b})y}(x) + u_{(\mathrm{s})y}(x)$ the coefficient d_0 may be set to zero without loss of generality. Polynomial coefficients meeting four prescribed end displacements and rotations, as well as internal equilibrium, provide the relations required to derive shape functions $\psi_2(x)$, $\psi_3(x)$, $\psi_5(x)$, and $\psi_6(x)$.

$$
\begin{aligned}
u_y(x) &= c_0 + c_1\left(\frac{x}{L}\right) + c_2\left(\frac{x}{L}\right)^2 + c_3\left(\frac{x}{L}\right)^3 + d_1\left(\frac{x}{L}\right) && (82)\\
&= \bar{u}_2\psi_2(x) + \bar{u}_3\psi_3(x) + \bar{u}_5\psi_5(x) + \bar{u}_6\psi_6(x). && (83)
\end{aligned}
$$

In prescribing the end conditions to find the c_i and d_i coefficients related to each $\psi_i(x)$, it is important to recognize that if $u_{(\mathrm{s})y}(x)$ is constant within the element, so that if $u_{(\mathrm{b})y}(0) = 0$ and $u_{(\mathrm{s})y}(0) = 0$, then there is not shear deformation within the element. Therefore, zero-rotation end conditions are prescribed only for the bending portion of the rotations as $u'_{(\mathrm{b})y}(0) = 0$. The derivitives involved in finding the polynomial coefficients are:

$$
\begin{aligned}
u'_{(\mathrm{b})y}(x) &= c_1\frac{1}{L} + 2c_2\frac{x}{L^2} + 3c_3\frac{x^2}{L^3} && (84)\\
u''_y(x) &= 2c_2\frac{1}{L^2} + 6c_3\frac{x}{L^3} && (85)\\
u'''_y(x) &= 6c_3\frac{1}{L^3} && (86)
\end{aligned}
$$

The fifth condition required to determine the five c_i and d_i coefficients is the internal equilibrium of the beam element,

$$
\begin{aligned}
\frac{d}{dx}M(x) &= -S && (87)\\
EIu'''_{(\mathrm{b})y} &= -GA_{(\mathrm{s})}u'_{(\mathrm{s})y} && (88)\\
EI(6c_3/L^3) &= -GA_{(\mathrm{s})}(d_1/L) && (89)\\
(\Phi/2)c_3 + d_1 &= 0 && (90)
\end{aligned}
$$

where $\Phi \equiv (12EI)/(GA_{(\mathrm{s})}L^2)$ is the ratio of bending stiffness to shear stiffness. If the shear stiffness is very large shear deformations are negligible. Shear deformations may be neglected by setting $\Phi = 0$. Expressions for the end displacements, end rotations, and internal equilibrium may be written in matrix form

$$
\begin{bmatrix} 1 & 0 & 0 & 0 & 0 \\ 0 & 1 & 0 & 0 & 0 \\ 1 & 1 & 1 & 1 & 1 \\ 0 & 1 & 2 & 3 & 0 \\ 0 & 0 & 0 & \Phi/2 & 1 \end{bmatrix}
\left\{ \begin{array}{c} c_0 \\ c_1 \\ c_2 \\ c_3 \\ d_1 \end{array} \right\}
=
\left\{ \begin{array}{c} u_y(0) \\ L\ u'_{(\mathrm{b})y}(0) \\ u_y(L) \\ L\ u'_{(\mathrm{b})y}(L) \\ M' + S \end{array} \right\}
\qquad (91)
$$

The end displacements and rotations corresponding to the four desired shape functions are:

	$\psi_{y2}(x)$	$\psi_{y3}(x)$	$\psi_{y5}(x)$	$\psi_{y6}(x)$
$u_y(0)$	1	0	0	0
$u'_{(\mathrm{b})y}(0)$	0	1	0	0
$u_y(L)$	0	0	1	0
$u'_{(\mathrm{b})y}(L)$	0	0	0	1
$M' + S$	0	0	0	0

The coefficients c_i and d_i for each shape function ψ_i may therefore be found from the first four columns of the inverse of the matrix in equation (91).

$$\left\{ \begin{array}{c} c_0 \\ c_1 \\ c_2 \\ c_3 \\ d_1 \end{array} \right\} = \frac{1}{1+\Phi} \left[\begin{array}{ccccc} 1+\Phi & 0 & 0 & 0 & 0 \\ 0 & 1+\Phi & 0 & 0 & 0 \\ -3 & -2-\Phi/2 & 3 & -1+\Phi/2 & -3 \\ 2 & 1 & -2 & 1 & 2 \\ -\Phi & -\Phi/2 & \Phi & -\Phi/2 & 1 \end{array} \right] \left\{ \begin{array}{c} u_y(0) \\ L\ u'_{(\mathrm{b})y}(0) \\ u_y(L) \\ L\ u'_{(\mathrm{b})y}(L) \\ M' + S \end{array} \right\} \tag{92}$$

After a little algebraic simplification, the shape functions satisfying the Timoshenko beam equations (equations (77), (78) and (79)) are,

$$\begin{aligned} \psi_{y2}(x) &= \tfrac{1}{1+\Phi}\left[1 - 3\left(\tfrac{x}{L}\right)^2 + 2\left(\tfrac{x}{L}\right)^3 + \left(1 - \tfrac{x}{L}\right)\Phi\right] \\ \psi_{y3}(x) &= \tfrac{L}{1+\Phi}\left[\tfrac{x}{L} - 2\left(\tfrac{x}{L}\right)^2 + \left(\tfrac{x}{L}\right)^3 + \tfrac{1}{2}\left(\tfrac{x}{L} - \left(\tfrac{x}{L}\right)^2\right)\Phi\right] \\ \psi_{y5}(x) &= \tfrac{1}{1+\Phi}\left[3\left(\tfrac{x}{L}\right)^2 - 2\left(\tfrac{x}{L}\right)^3 + \tfrac{x}{L}\ \Phi\right] \\ \psi_{y6}(x) &= \tfrac{L}{1+\Phi}\left[-\left(\tfrac{x}{L}\right)^2 + \left(\tfrac{x}{L}\right)^3 - \tfrac{1}{2}\left(\tfrac{x}{L} - \left(\tfrac{x}{L}\right)^2\right)\Phi\right] \end{aligned} \tag{93}$$

The term Φ gives the relative importance of the shear deformations to the bending deformations,

$$\Phi = \frac{12EI}{G(A/\alpha)L^2} = 24\alpha(1+\nu)\left(\frac{r}{L}\right)^2 , \tag{94}$$

where r is the "radius of gyration" of the cross section, $r = \sqrt{I/A}$, and ν is Poisson's ratio. Shear deformation effects are significant for beams which have a length-to-depth ratio less than 5. To neglect shear deformation, set $\Phi = 0$. These displacement functions are exact for frame elements with constant shear forces S and linearly varying bending moment distributions, $M(x)$, in which the strain energy has both a shear stress component and a normal stress component,

$$U = \frac{1}{2}\int_0^L EI\left(\sum_{n=1}^{6} \psi''_{(\mathrm{b})yn}(x)\bar{u}_n\right)^2 dx + \frac{1}{2}\int_0^L G(A/\alpha)\left(\sum_{n=1}^{6} \psi'_{(\mathrm{s})yn}(x)\bar{u}_n\right)^2 dx \tag{95}$$

The Timoshenko beam shape functions (93) represent the combination of bending shape functions $\psi_{(\mathrm{b})}(x)$ and shear shape functions $\psi_{\mathrm{s}}(s)$. This document demonstrates the decomposition of the shape functions into components associated with bending deformation

$\psi_{(b)yn}(x)$ and shear deformation, $\psi_{(s)yn}(x)$ using symmetry arguments to decompose $\psi_{y2}(x)$ into $\psi_{(b)y2}(x)$ and $\psi_{(s)y2}(x)$ and using Castigliano's Second Theorem and superposition to decompose $\psi_{y3}(x)$ into $\psi_{(b)y3}(x)$ and $\psi_{(s)y3}(x)$. Shape functions $\psi_{y5}(x)$ and $\psi_{y6}(x)$ are decomposed in an analogous way.

Using symmetry to decompose shape function $\psi_2(x)$, the end moments M_1 and M_2 in (78) must be equal to each other; the end shears must be twice this moment divided by the length. Without loss of generality, and for convenience, we assign $M_1 = M_2 = 6EI/L^2$ and $V_1 = V_2 = 12EI/L^3$. Integrating (78) twice, with $M(x) = (6EI/L^2)(2x/L - 1)$ and with boundary conditions $u_{(b)}(0) = 1$, $u_{(b)}(L) = 0$, $u'_{(b)}(0) = 0$, and $u'_{(b)}(L) = 0$ we obtain

$$u_{(b)}(x) = 1 - 3\left(\frac{x}{L}\right)^2 + 2\left(\frac{x}{L}\right)^3 .$$

Integrating (79) once with $V(x) = 12EI/L^3$ and with boundary condition $u_{(s)}(L) = 0$ we obtain

$$u_{(s)}(x) = \Phi\left[1 - \frac{x}{L}\right] .$$

The shape function $\psi_{y2}(x)$ is obtained by superposing $u_{(b)y}(x)$ and $u_{(s)y}(x)$ and normalizing so that $\psi_{y2}(0) = 1$.

Likewise, to decompose shape function $\psi_5(x)$, the end moments M_1 and M_2 in (78) must be equal to each other; the end shears must be twice this moment divided by the length. Without loss of generality, and for convenience, we assign $M_1 = M_2 = -6EI/L^2$ and $V_1 = V_2 = -12EI/L^3$. Integrating (78) twice, with $M(x) = (6EI/L^2)(1-2x/L)$ $u_{(b)}(L) = 1$ and $u'_{(b)}(L) = 0$ we obtain

$$u_{(b)}(x) = 3\left(\frac{x}{L}\right)^2 - 2\left(\frac{x}{L}\right)^3 .$$

Integrating (79) once with $V(x) = -12EI/L^3$ and with boundary condition $u_{(s)}(0) = 0$, we obtain

$$u_{(s)}(x) = \Phi\left[\frac{x}{L}\right] .$$

The shape function $\psi_{y2}(x)$ is obtained by superposing $u_{(b)y}(x)$ and $u_{(s)y}(x)$ and normalizing so that $\psi_{y5}(L) = 1$.

Before continuing we note that the quadratic and cubic terms of the Timoshenko shape functions $\psi_{y2}(x)$ and $\psi_{y5}(x)$ are allocated to the bending portion of the shape function while the linear terms are allocated to the shear portion. The following shows that this allocation based on the order of the terms does not hold for $\psi_{y3}(x)$ and $\psi_{y6}(x)$.

Shape functions $\psi_{y3}(x)$ and $\psi_{y6}(x)$ do not have the symmetry of $\psi_{y2}(x)$ and $\psi_{y5}(x)$. Here, the decomposing of $\psi_{y3}(x)$ and $\psi_{y6}(x)$ into bending and shear components is accomplished via superposition and Castigliano's Theorem.

For $\psi_{y3}(x)$ the beam is loaded, for convenience with $M_1 = 4EI/L$ and the indeterminate reaction is chosen as $V_1 = V(0)$ and is solved for via Castigliano's Second Theorem and the criterion that the displacement collocated with V_1 is zero.

Expressing the internal moment and shear as a superposition of moments and shears in equilibrium with M_1 and a unit transverse load collocated with V_1, we obtain the superposition expressions $M(x) = M_o(x) + m(x)V_1$ and $V(x) = V_o(x) + v(x)V_1$. where $M_o(x) = 4EI/L$, $m(x) = x$, $V_o(x) = 0$ and $v(x) = -1$. The strain energy here is

$$U = \frac{1}{2}\frac{1}{EI}\int_0^L M^2(x)\;dx + \frac{1}{2}\frac{1}{GA/\alpha}\int_0^L V^2(x)\;dx\;.$$

Via Castigliano's Second Theorem,

$$\frac{\partial U}{\partial V_1} = 0 = \frac{1}{EI}\int_0^L (M_o(x) + m(x)V_1)m(x)\;dx + \frac{1}{GA/\alpha}\int_0^L (V_o(x) + v(x)V_1)v(x)\;dx\;.$$

Solving this expression for V_1 gives

$$V_1 = \frac{6EI}{L^2}\frac{1}{1+\Phi/4}\;.$$

Substituting this expression of V_1 into the superposition expression for the internal moment and shear we obtain,

$$M(x) = -\frac{4EI}{L} + \frac{6EI}{L^2}\frac{1}{1+\Phi/4}\;x$$

and

$$V(x) = \frac{6EI}{L^2}\frac{1}{1+\Phi/4}.$$

Integrating (78) twice, with $M(x)$ (as given above) and with the boundary condition $u'_{(\mathrm{b})}(L) = 0$ we obtain

$$u_{(\mathrm{b})}(x) = \frac{1}{1+\Phi/4}\left[\frac{x}{L} - 2\left(\frac{x}{L}\right)^2 + \left(\frac{x}{L}\right)^3 + \frac{1}{2}\Phi\left(2\frac{x}{L} - \left(\frac{x}{L}\right)^2\right)\right]L\;.$$

Integrating (79) once with $V(x)$ (as given above) and with boundary condition $u_{(\mathrm{s})}(L) = 0$, we obtain

$$u_{(\mathrm{s})}(x) = -\frac{1}{2}\frac{\Phi}{1+\Phi/4}\;x\;.$$

The shape function $\psi_{y3}(x)$ is obtained by superposing $u_{(\mathrm{b})y}(x)$ and $u_{(\mathrm{s})y}(x)$ and normalizing so that $\psi'_{(\mathrm{b})y3}(0) = 1$.

Likewise, for $\psi_{y6}(x)$ the beam is loaded, for convenience with $M_2 = 4EI/L$ and the indeterminate reaction is chosen as $V_2 = V(L)$ and is solved for via Castigliano's Second Theorem and the criterion that the displacement collocated with V_2 is zero. By direct analogy to the preceding, we can confidently state

$$V_2 = \frac{6EI}{L^2}\frac{1}{1+\Phi/4}\;.$$

Substituting this expression of V_2 into the superposition expression for the internal moment and shear we obtain,

$$M(x) = \frac{4EI}{L} + \frac{6EI}{L^2}\frac{1}{1+\Phi/4}\ (x-L)$$

and

$$V(x) = -\frac{6EI}{L^2}\frac{1}{1+\Phi/4}.$$

Integrating (78) twice, with $M(x)$ (as given above) and with boundary conditions $u'_{(\mathrm{b})}(0) = 0$ we obtain

$$u_{(\mathrm{b})}(x) = \frac{1}{1+\Phi/4}\left[-\left(\frac{x}{L}\right)^2 + \left(\frac{x}{L}\right)^3 + \frac{1}{2}\Phi\left(\left(\frac{x}{L}\right)^2\right)\right] L\ .$$

Integrating (79) once with $V(x)$ (as given above) and with boundary condition $u_{(\mathrm{s})}(0) = 0$, we obtain

$$u_{(\mathrm{s})}(x) = -\frac{1}{2}\frac{\Phi}{1+\Phi/4}\ x\ .$$

The shape function $\psi_{y6}(x)$ is obtained by superposing $u_{(\mathrm{b})y}(x)$ and $u_{(\mathrm{s})y}(x)$ and normalizing so that $\psi'_{(\mathrm{b})y6}(L) = 1$.

The resulting set of Timoshenko beam shape functions, decomposed into bending and shear components is:

$$\begin{aligned}
\psi_{(\mathrm{b})y2}(x) &= \frac{1}{1+\Phi}\left[1 - 3\left(\frac{x}{L}\right)^2 + 2\left(\frac{x}{L}\right)^3\right] \\
\psi_{(\mathrm{s})y2}(x) &= \frac{\Phi}{1+\Phi}\left[1 - \frac{x}{L}\right] \\
\psi_{(\mathrm{b})y3}(x) &= \frac{L}{1+\Phi}\left[\frac{x}{L} - 2\left(\frac{x}{L}\right)^2 + \left(\frac{x}{L}\right)^3 + \frac{1}{2}\left(2\frac{x}{L} - \left(\frac{x}{L}\right)^2\right)\Phi\right] \\
\psi_{(\mathrm{s})y3}(x) &= -\frac{L\Phi}{1+\Phi}\left[\frac{1}{2}\frac{x}{L}\right] \\
\psi_{(\mathrm{b})y5}(x) &= \frac{1}{1+\Phi}\left[3\left(\frac{x}{L}\right)^2 - 2\left(\frac{x}{L}\right)^3\right] \\
\psi_{(\mathrm{s})y5}(x) &= \frac{\Phi}{1+\Phi}\left[\frac{x}{L}\right] \\
\psi_{(\mathrm{b})y6}(x) &= \frac{L}{1+\Phi}\left[-\left(\frac{x}{L}\right)^2 + \left(\frac{x}{L}\right)^3 + \frac{1}{2}\left(\left(\frac{x}{L}\right)^2\right)\Phi\right] \\
\psi_{(\mathrm{s})y6}(x) &= -\frac{L}{1+\Phi}\left[\frac{1}{2}\frac{x}{L}\Phi\right]
\end{aligned}$$

The superposition of each pair of bending and shear component is consistent with the independently derived Timoshenko shape functions in (93).

4.2 Timoshenko Beam Element Stiffness Matrices

The elastic and geometric stiffness matrices for a Timoshenko beam element may be derived as was done with the Bernoulli-Euler beam element, but using separate shape functions for bending deformation and shear deformation,

$$\begin{aligned} \bar{K}_{ij} = \quad & EA \quad \int_0^L \psi'_{xi}(x)\psi'_{xj}(x)\; dx \\ + \quad & EI \quad \int_0^L \psi''_{(\mathrm{b})yi}(x)\psi''_{(\mathrm{b})yj}(x)\; dx \\ + \quad & G(A/\alpha) \quad \int_0^L \psi'_{(\mathrm{s})yi}(x)\psi'_{(\mathrm{s})yj}(x)\; dx \\ + \quad & N \quad \int_0^L \psi'_{yi}(x)\psi'_{yj}(x)\; dx \end{aligned} \tag{96}$$

where the displacement shape functions $\psi_{xn}(x)$ are given in (37), $\psi_{yn}(x)$ are given in (93), $\psi_{(\mathrm{b})yn}(x)$ and $\psi_{(\mathrm{s})yn}(x)$ are provided in section 4.1.

4.3 Timoshenko Beam Element Mass Matrices

The mass matrix for a Timoshenko beam element need not distinguish between bending and shear effects.

$$\begin{aligned} \bar{M}_{ij} = \quad & \rho A \quad \int_0^L \psi_{xi}(x)\psi_{xj}(x)\; dx \\ + \quad & \rho A \quad \int_0^L \psi_{yi}(x)\psi_{yj}(x)\; dx \end{aligned} \tag{97}$$

where the shape functions $\psi_{xn}(x)$ are given in (37) and $\psi_{yn}(x)$ are given in (93).

4.4 Timoshenko Beam Element Stiffness and Mass Matrices, (including shear deformation effects but not rotatory inertia)

For prismatic homogeneous isotropic beams, substituting the previous expressions for the functions $\psi_{xn}(x)$ and $\psi_{(\mathrm{b})yn}(x)$, and $\psi_{(\mathrm{s})yn}(x)$ into equation (96) and (97), results in the Timoshenko element elastic stiffness matrices $\bar{\boldsymbol{K}}_\mathrm{e}$, mass matrix $\bar{\boldsymbol{M}}$, and geometric stiffness matrix $\bar{\boldsymbol{K}}_\mathrm{g}$

$$\bar{\boldsymbol{M}} = \frac{\rho A L}{840}\begin{bmatrix} 280 & 0 & 0 & 140 & 0 & 0 \\ & 312+588\Phi+280\Phi^2 & (44+77\Phi+35\Phi^2)L & 0 & 108+252\Phi+175\Phi^2 & -(26+63\Phi+35\Phi^2)L \\ & & (8+14\Phi+7\Phi^2)L^2 & 0 & (26+63\Phi+35\Phi^2)L & -(6+14\Phi+7\Phi^2)L^2 \\ & & & 280 & 0 & 0 \\ & \mathrm{SYM} & & & 312+588\Phi+280\Phi^2 & -(44+77\Phi+35\Phi^2)L \\ & & & & & (8+14\Phi+7\Phi^2)L^2 \end{bmatrix} \tag{98}$$

$$\bar{\boldsymbol{K}}_\mathrm{e} = \begin{bmatrix} \frac{EA}{L} & 0 & 0 & -\frac{EA}{L} & 0 & 0 \\ & \frac{12}{1+\Phi}\frac{EI}{L^3} & \frac{6}{1+\Phi}\frac{EI}{L^2} & 0 & -\frac{12}{1+\Phi}\frac{EI}{L^3} & \frac{6}{1+\Phi}\frac{EI}{L^2} \\ & & \frac{4+\Phi}{1+\Phi}\frac{EI}{L} & 0 & -\frac{6}{1+\Phi}\frac{EI}{L^2} & \frac{2-\Phi}{1+\Phi}\frac{EI}{L} \\ & & & \frac{EA}{L} & 0 & 0 \\ & \mathrm{SYM} & & & \frac{12}{1+\Phi}\frac{EI}{L^3} & -\frac{6}{1+\Phi}\frac{EI}{L^2} \\ & & & & & \frac{4+\Phi}{1+\Phi}\frac{EI}{L} \end{bmatrix} \tag{99}$$

$$\bar{\boldsymbol{K}}_\mathrm{g} = \frac{N}{L}\begin{bmatrix} 0 & 0 & 0 & 0 & 0 & 0 \\ & \frac{6/5+2\Phi+\Phi^2}{(1+\Phi)^2} & \frac{L/10}{(1+\Phi)^2} & 0 & \frac{-6/5-2\Phi-\Phi^2}{(1+\Phi)^2} & \frac{L/10}{(1+\Phi)^2} \\ & & \frac{2L^2/15+L^2\Phi/6+L^2\Phi^2/12}{(1+\Phi)^2} & 0 & \frac{-L/10}{(1+\Phi)^2} & \frac{-L^2/30-L^2\Phi/6-L^2\Phi^2/12}{(1+\Phi)^2} \\ & & & 0 & 0 & 0 \\ & \mathrm{SYM} & & & \frac{6/5+2\Phi+\Phi^2}{(1+\Phi)^2} & \frac{-L/10}{(1+\Phi)^2} \\ & & & & & \frac{2L^2/15+L^2\Phi/6+L^2\Phi^2/12}{(1+\Phi)^2} \end{bmatrix} \tag{100}$$

4.5 Timoshenko Beam Element Mass Matrix (including rotatory inertia but not shear deformation effects)

Consider again the geometry of a deformed beam with linearly-varying axial beam displacements outside of the neutral axis. The functions $u_x(x, y)$ and $u_y(x, y)$ now describe the

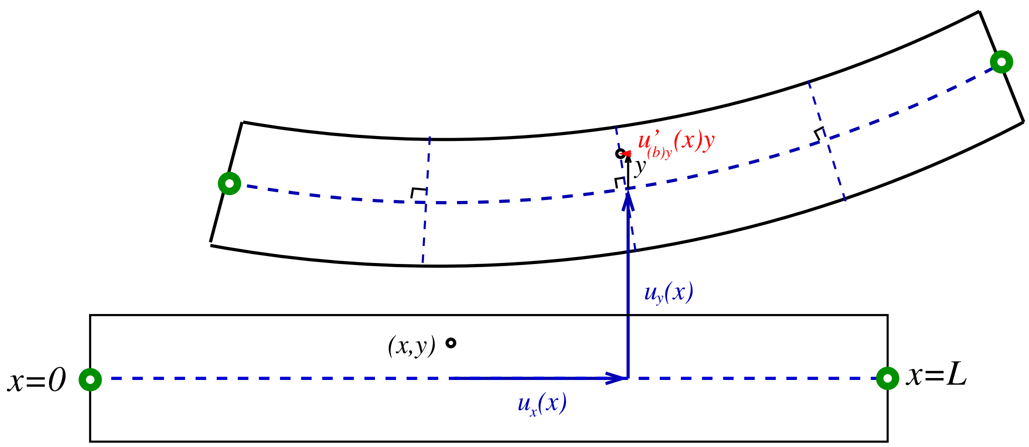

Figure 10. Deformation of beam element showing axial-direction displacements $u_x(x, y, t)$ outside the neutral axis due to bending.

translation of points anywhere within the beam, as a function of the location within the beam. The internal displacements $u_x(x, y, t)$ and $u_y(x, y, t)$ are expressed in terms of a set of shape functions, $\psi_{xn}(x, y)$ and $\psi_{yn}(x)$, and the end displacements $(\bar{u}_1(t), \bar{u}_2(t), \bar{u}_4(t), \bar{u}_5(t))$ and the end rotations $(\bar{u}_3(t), \bar{u}_6(t))$.

$$
\begin{aligned}
u_x(x, y, t) &= \sum_{n=1}^{6} \psi_{xn}(x, y)\ \bar{u}_n(t) \\
u_y(x, t) &= \sum_{n=1}^{6} \psi_{yn}(x)\ \bar{u}_n(t)
\end{aligned}
$$

The shape functions for transverse displacements $\psi_{yn}(x)$ are the same as the shape functions $\psi_{yn}(x)$ for the Bernouli-Euler beam. The shape functions for axial displacements along the neutral axis, $\psi_{x1}(x, y)$ and $\psi_{x4}(x, y)$ are also the same as the shape functions $\psi_{x1}(x)$ and $\psi_{x4}(x)$ used previously. To account for axial displacements outside of the neutral axis, four new shape functions are derived from the assumption that plane sections remain plane,

$u_x(x,y) = -u'_{(\mathrm{b})y}(x) y$.

$$
\begin{aligned}
\psi_{x2}(x,y) &= -\psi'_{(\mathrm{b})y2}\; y = & 6\left(\frac{x}{L} - \left(\frac{x}{L}\right)^2\right)\frac{y}{L} \\
\psi_{x3}(x,y) &= -\psi'_{(\mathrm{b})y3}\; y = & \left(-1 + 4\frac{x}{L} - 3\left(\frac{x}{L}\right)^2\right) y \\
\psi_{x5}(x,y) &= -\psi'_{(\mathrm{b})y5}\; y = & 6\left(-\frac{x}{L} + \left(\frac{x}{L}\right)^2\right)\frac{y}{L} \\
\psi_{x6}(x,y) &= -\psi'_{(\mathrm{b})y6}\; y = & \left(2\frac{x}{L} - 3\left(\frac{x}{L}\right)^2\right) y
\end{aligned}
$$

Because ψ_{yn}, ψ_{x1} and ψ_{x4} are unchanged, the stiffness matrix is also unchanged.

Evaluating equation (30) using the new shape functions ψ_{x2}, ψ_{x3}, ψ_{x5}, and ψ_{x6}, results in a mass matrix incorporating rotatory inertia.

$$
\bar{\boldsymbol{M}} = \rho A L \begin{bmatrix}
\frac{1}{3} & 0 & 0 & \frac{1}{6} & 0 & 0 \\
 & \frac{13}{35} + \frac{6}{5}\frac{r^2}{L^2} & \frac{11}{210}L + \frac{1}{10}\frac{r^2}{L} & 0 & \frac{9}{70} - \frac{6}{5}\frac{r^2}{L^2} & -\frac{13}{420}L + \frac{1}{10}\frac{r^2}{L} \\
 & & \frac{1}{105}L^2 + \frac{2}{15}r^2 & 0 & \frac{13}{420}L + \frac{1}{10}\frac{r^2}{L} & 0 \\
 & \text{SYM} & & \frac{1}{3} & 0 & 0 \\
 & & & & \frac{13}{35} + \frac{6}{5}\frac{r^2}{L^2} & -\frac{11}{210}L + \frac{1}{10}\frac{r^2}{L} \\
 & & & & & \frac{1}{105}L^2 + \frac{2}{15}r^2
\end{bmatrix} \tag{101}
$$

Beam element mass matrices including the effects of shear deformation on rotatory inertia are more complicated. Refer to p 295 of *Theory of Matrix Structural Analysis,* by J.S. Przemieniecki (Dover Pub., 1985).

5 Coordinate Transformation for Beam Elements

5.1 Bernoulli-Euler Beam Element Stiffness Matrix in Local Element Coordinates, $\bar{\boldsymbol{K}}$

$$\bar{\boldsymbol{f}} = \bar{\boldsymbol{K}}\ \bar{\boldsymbol{u}}$$

$$\left\{ \begin{array}{c} N_1 \\ S_1 \\ M_1 \\ N_2 \\ S_2 \\ M_2 \end{array} \right\} = \left[\begin{array}{cccccc} \frac{EA}{L} & 0 & 0 & -\frac{EA}{L} & 0 & 0 \\ 0 & \frac{12EI}{L^3} & \frac{6EI}{L^2} & 0 & -\frac{12EI}{L^3} & \frac{6EI}{L^2} \\ 0 & \frac{6EI}{L^2} & \frac{4EI}{L} & 0 & -\frac{6EI}{L^2} & \frac{2EI}{L} \\ -\frac{EA}{L} & 0 & 0 & \frac{EA}{L} & 0 & 0 \\ 0 & -\frac{12EI}{L^3} & -\frac{6EI}{L^2} & 0 & \frac{12EI}{L^3} & -\frac{6EI}{L^2} \\ 0 & \frac{6EI}{L^2} & \frac{2EI}{L} & 0 & -\frac{6EI}{L^2} & \frac{4EI}{L} \end{array} \right] \left\{ \begin{array}{c} \Delta_{1x} \\ \Delta_{1y} \\ \theta_{1z} \\ \Delta_{2x} \\ \Delta_{2y} \\ \theta_{2z} \end{array} \right\}$$

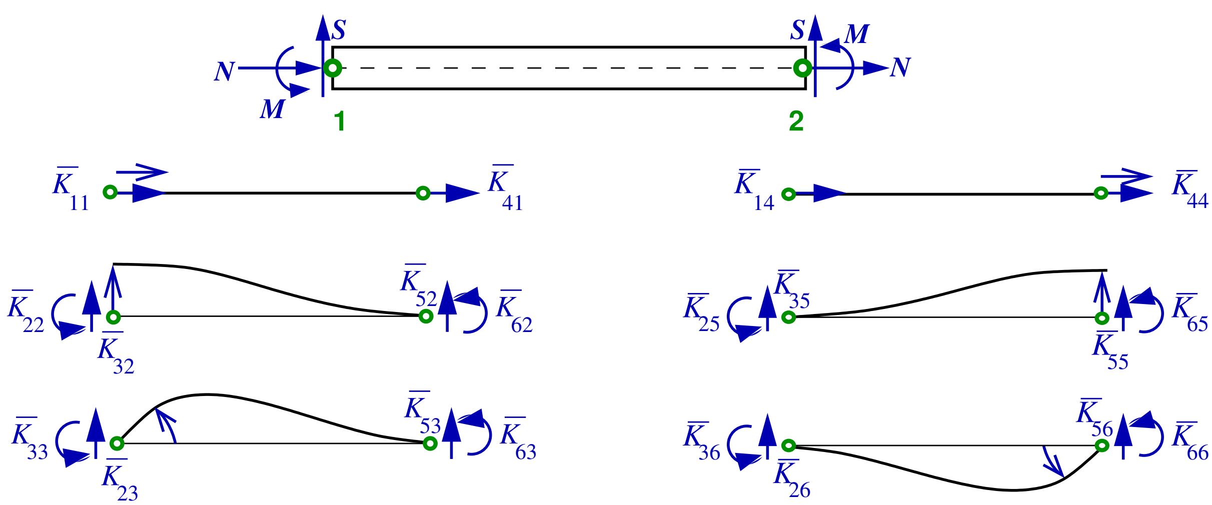

Figure 11. Column j of the stiffness matrix are the set of forces associated with a unit displacement or rotation at coordinate j (only).

5.2 Beam Element Stiffness Matrix in Global Coordinates, $\mathbf{K}$

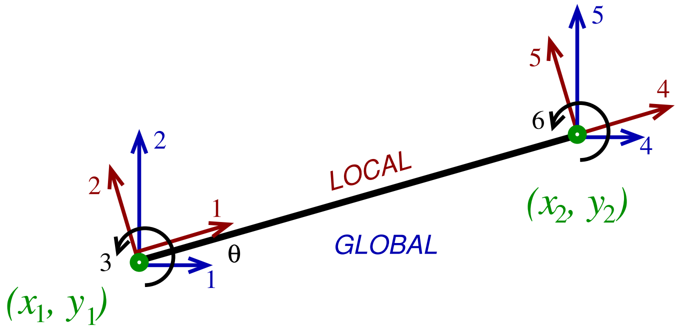

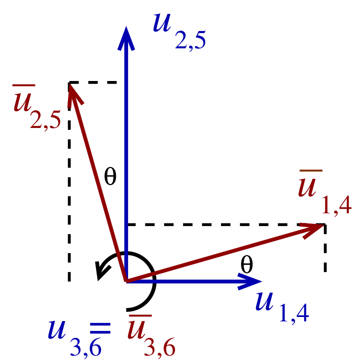

Transformation from local element coordinates $(\bar{\boldsymbol{u}}, \bar{\boldsymbol{f}})$ to global element coordinates $(\boldsymbol{u}, \boldsymbol{f})$

node1 : $\quad u_1 = \bar{u}_1 \cos\theta - \bar{u}_2 \sin\theta \qquad u_2 = \bar{u}_1 \sin\theta + \bar{u}_2 \cos\theta \qquad u_3 = \bar{u}_3$

node2 : $\quad u_4 = \bar{u}_4 \cos\theta - \bar{u}_5 \sin\theta \qquad u_5 = \bar{u}_4 \sin\theta + \bar{u}_5 \cos\theta \qquad u_6 = \bar{u}_6$

$$\boldsymbol{T} = \begin{bmatrix} c & -s & 0 & & & \\ s & c & 0 & & 0 & \\ 0 & 0 & 1 & & & \\ & & & c & -s & 0 \\ & 0 & & s & c & 0 \\ & & & 0 & 0 & 1 \end{bmatrix} \qquad c = \cos\theta = \frac{x_2 - x_1}{L} \qquad s = \sin\theta = \frac{y_2 - y_1}{L}$$

$$\boldsymbol{T}^{\mathsf{T}}\boldsymbol{T} = \boldsymbol{I} \qquad \boldsymbol{u} = \boldsymbol{T}\ \bar{\boldsymbol{u}} \qquad \boldsymbol{f} = \boldsymbol{T}\ \bar{\boldsymbol{f}}$$

Element stiffness matrix in global coordinates: $\boldsymbol{K} = \boldsymbol{T}\ \bar{\boldsymbol{K}}\ \boldsymbol{T}^{\mathsf{T}}$

$$\boldsymbol{K} = \begin{bmatrix}
\frac{EA}{L}c^2 + \frac{12EI}{L^3}s^2 & \frac{EA}{L}cs - \frac{12EI}{L^3}cs & -\frac{6EI}{L^2}s & -\frac{EA}{L}c^2 - \frac{12EI}{L^3}s^2 & -\frac{EA}{L}cs + \frac{12EI}{L^3}cs & -\frac{6EI}{L^2}s \\
 & \frac{EA}{L}s^2 + \frac{12EI}{L^3}c^2 & \frac{6EI}{L^2}c & -\frac{EA}{L}cs + \frac{12EI}{L^3}cs & -\frac{EA}{L}s^2 - \frac{12EI}{L^3}c^2 & \frac{6EI}{L^2}c \\
 & & \frac{4EI}{L} & \frac{6EI}{L^2}s & -\frac{6EI}{L^2}c & \frac{2EI}{L} \\
 & & & \frac{EA}{L}c^2 + \frac{12EI}{L^3}s^2 & \frac{EA}{L}cs - \frac{12EI}{L^3}cs & \frac{6EI}{L^2}s \\
 & \text{SYM} & & & \frac{EA}{L}s^2 + \frac{12EI}{L^3}c^2 & -\frac{6EI}{L^2}c \\
 & & & & & \frac{4EI}{L}
\end{bmatrix}$$

$$\boldsymbol{f} = \boldsymbol{K}\ \boldsymbol{u}$$

5.3 Beam Element Consistent Mass Matrix in Local Element Coordinates, $\bar{\boldsymbol{M}}$

$$\bar{\boldsymbol{f}} = \bar{\boldsymbol{M}}\ \ddot{\bar{\boldsymbol{u}}}$$

$$\left\{ \begin{array}{c} N_1 \\ V_1 \\ M_1 \\ N_2 \\ V_2 \\ M_2 \end{array} \right\} = \frac{\rho A L}{420} \left[\begin{array}{cccccc} 140 & 0 & 0 & 70 & 0 & 0 \\ 0 & 156 & 22L & 0 & 54 & -13L \\ 0 & 22L & 4L^2 & 0 & 13L & -3L^2 \\ 70 & 0 & 0 & 140 & 0 & 0 \\ 0 & 54 & 13L & 0 & 156 & -22L \\ 0 & -13L & -3L^2 & 0 & -22L & 4L^2 \end{array} \right] \left\{ \begin{array}{c} \ddot{\bar{u}}_1 \\ \ddot{\bar{u}}_2 \\ \ddot{\bar{u}}_3 \\ \ddot{\bar{u}}_4 \\ \ddot{\bar{u}}_5 \\ \ddot{\bar{u}}_6 \end{array} \right\}$$

For beam element mass matrices including shear deformations, see:
Theory of Matrix Structural Analysis, by J.S. Przemieniecki
(Dover Pub., 1985). (... a steal at $12.95)

5.4 Beam Element Consistent Mass Matrix in Global Coordinates, $\mathbf{M}$

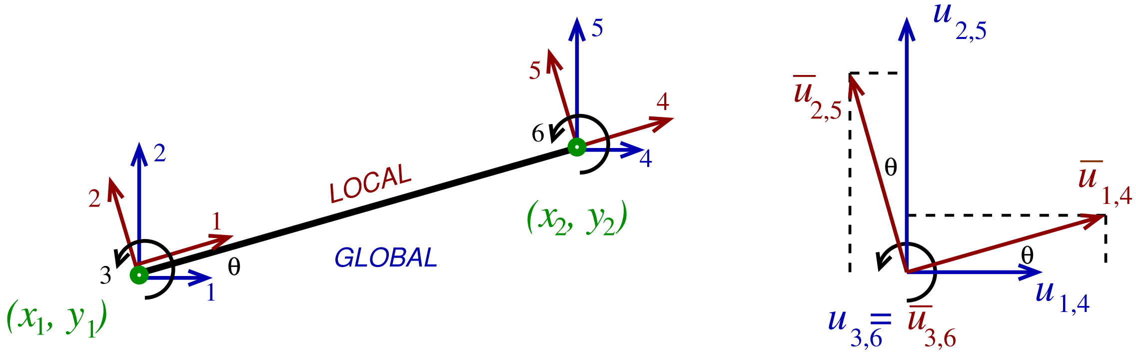

Transformation from local element coordinates $(\bar{\boldsymbol{u}}, \bar{\boldsymbol{f}})$ to global element coordinates $(\boldsymbol{u}, \boldsymbol{f})$

node1 : $u_1 = \bar{u}_1 \cos\theta - \bar{u}_2 \sin\theta$ $\quad u_2 = \bar{u}_1 \sin\theta + \bar{u}_2 \cos\theta$ $\quad u_3 = \bar{u}_3$

node2 : $u_4 = \bar{u}_4 \cos\theta - \bar{u}_5 \sin\theta$ $\quad u_5 = \bar{u}_4 \sin\theta + \bar{u}_5 \cos\theta$ $\quad u_6 = \bar{u}_6$

$$\boldsymbol{T} = \left[\begin{array}{cccccc} c & -s & 0 & & & \\ s & c & 0 & & 0 & \\ 0 & 0 & 1 & & & \\ & & & c & -s & 0 \\ & 0 & & s & c & 0 \\ & & & 0 & 0 & 1 \end{array}\right]$$

$$c = \cos\theta = \frac{x_2 - x_1}{L} \qquad s = \sin\theta = \frac{y_2 - y_1}{L}$$

$$\boldsymbol{T}^{\mathsf{T}}\boldsymbol{T} = \boldsymbol{I} \qquad \boldsymbol{u} = \boldsymbol{T}\ \bar{\boldsymbol{u}} \qquad \boldsymbol{f} = \boldsymbol{T}\ \bar{\boldsymbol{f}}$$

Element consistent mass matrix in global coordinates: $\boldsymbol{M} = \boldsymbol{T}\ \bar{\boldsymbol{M}}\ \boldsymbol{T}^{\mathsf{T}}$

$$\boldsymbol{M} = \frac{\rho A L}{420} \left[\begin{array}{cccccc} 140c^2 + 15s^2 & -16cs & -22sL & 70c^2 + 54s^2 & 16cs & 13sL \\ & 140s^2 + 156c^2 & 22cL & 16cs & 70s^2 + 54c^2 & -13cL \\ & & 4L^2 & -13sL & 13cL & -3L^2 \\ & & & 140c^2 + 156s^2 & -16cs & 22sL \\ & \text{SYM} & & & 140s^2 + 156c^2 & -22cL \\ & & & & & 4L^2 \end{array}\right]$$

$$\boldsymbol{f} = \boldsymbol{M}\ \ddot{\boldsymbol{u}}$$

6 2D Plane-Stress and Plane-Strain Rectangular Element Matrices

2D, isotropic, homogeneous element, with uniform thickness h.

Approximate element stiffness and mass matrices based on assumed distribution of internal displacements.

6.1 2D Rectangular Element Coordinates and Internal Displacements

Consider the geometry of a rectangle with edges aligned with a Cartesian coordinate system. $(0 \le x \le a,\ 0 \le y \le b)$ The functions $u_x(x, y, t)$ and $u_y(x, y, t)$ describe the in-plane displacements as a function of the location within the element.

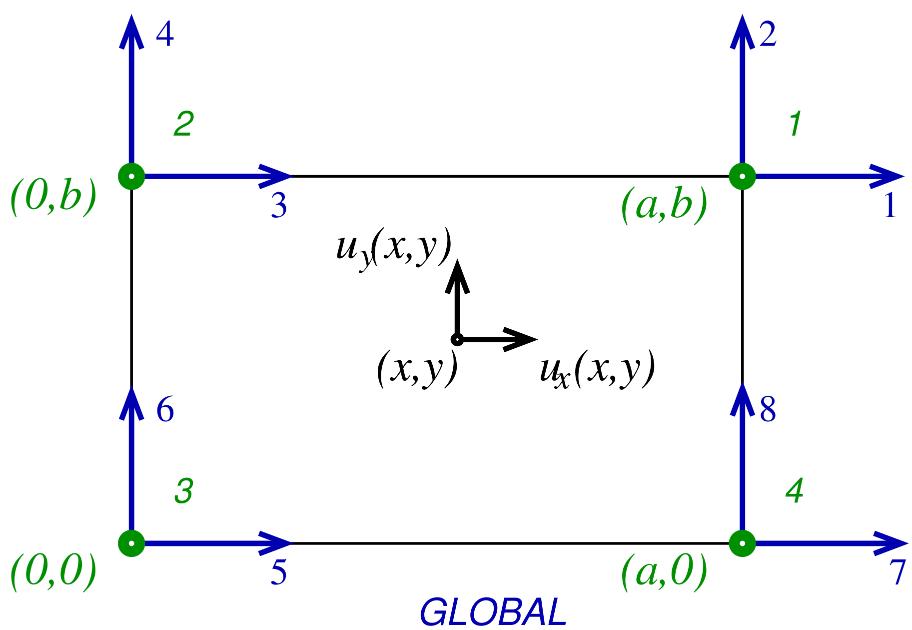

Figure 12. 2D rectangular element coordinates and displacements.

Internal displacements are assumed to vary linearly within the element.

$$\begin{aligned} u_x(x, y, t) &= c_1 \frac{x}{a} + c_2 \frac{x}{a}\frac{y}{b} + c_3 \frac{y}{b} + c_4 \\ u_y(x, y, t) &= c_5 \frac{x}{a} + c_6 \frac{x}{a}\frac{y}{b} + c_7 \frac{y}{b} + c_8 \end{aligned}$$

The eight coefficients $c_1, \cdots, c_8$ may be found uniquely from matching the displacement coordinates at the corners.

$$\begin{array}{lcl} u_x(a, b) = \bar{u}_1 & , & u_y(a, b) = \bar{u}_2 \\ u_x(0, b) = \bar{u}_3 & , & u_y(0, b) = \bar{u}_4 \\ u_x(0, 0) = \bar{u}_5 & , & u_y(0, 0) = \bar{u}_6 \\ u_x(a, 0) = \bar{u}_7 & , & u_y(a, 0) = \bar{u}_8 \end{array}$$

resulting in internal displacements

$$u_x(x,y,t) = \hat{x}\hat{y}\ \bar{u}_1(t) + (1-\hat{x})\hat{y}\ \bar{u}_3(t) + (1-\hat{x})(1-\hat{y})\ \bar{u}_5(t) + \hat{x}(1-\hat{y})\ \bar{u}_7(t) \quad (102)$$
$$u_y(x,y,t) = \hat{x}\hat{y}\ \bar{u}_2(t) + (1-\hat{x})\hat{y}\ \bar{u}_4(t) + (1-\hat{x})(1-\hat{y})\ \bar{u}_6(t) + \hat{x}(1-\hat{y})\ \bar{u}_8(t) \quad (103)$$

where $\hat{x} = x/a$ $(0 \le \hat{x} \le 1)$ and $\hat{y} = y/b$ $(0 \le \hat{y} \le 1)$ so that

$$\boldsymbol{\Psi}(\hat{x},\hat{y}) = \left[\begin{array}{c|c|c|c|c|c|c|c} \hat{x}\hat{y} & 0 & (1-\hat{x})\hat{y} & 0 & (1-\hat{x})(1-\hat{y}) & 0 & \hat{x}(1-\hat{y}) & 0 \\ \hline 0 & \hat{x}\hat{y} & 0 & (1-\hat{x})\hat{y} & 0 & (1-\hat{x})(1-\hat{y}) & 0 & \hat{x}(1-\hat{y}) \end{array}\right] \quad (104)$$

and

$$\left[\begin{array}{c} u_x(\hat{x},\hat{y},t) \\ u_y(\hat{x},\hat{y},t) \end{array}\right] = \boldsymbol{\Psi}(\hat{x},\hat{y})\ \bar{\boldsymbol{u}}(t) \quad (105)$$

Strain-displacement relations

$$\begin{aligned} \epsilon_{xx} &= \frac{\partial u_x}{\partial x} = \frac{1}{a}\frac{\partial u_x}{\partial \hat{x}} \\ \epsilon_{yy} &= \frac{\partial u_y}{\partial y} = \frac{1}{b}\frac{\partial u_y}{\partial \hat{y}} \\ \gamma_{xy} &= \frac{\partial u_x}{\partial y} + \frac{\partial u_y}{\partial x} = \frac{1}{b}\frac{\partial u_x}{\partial \hat{y}} + \frac{1}{a}\frac{\partial u_y}{\partial \hat{x}} \end{aligned}$$

so that

$$\left\{\begin{array}{c} \epsilon_{xx} \\ \epsilon_{yy} \\ \gamma_{xy} \end{array}\right\} = \left[\begin{array}{cccccccc} \hat{y}/a & 0 & -\hat{y}/a & 0 & -(1-\hat{y})/a & 0 & (1-\hat{y})/a & 0 \\ 0 & \hat{x}/b & 0 & (1-\hat{x})/b & 0 & -(1-\hat{x})/b & 0 & -\hat{x}/b \\ \hat{x}/b & \hat{y}/a & (1-\hat{x})/b & -\hat{y}/a & -(1-\hat{x})/b & -(1-\hat{y})/a & -\hat{x}/b & (1-\hat{y})/a \end{array}\right] \left\{\begin{array}{c} \bar{u}_1 \\ \bar{u}_2 \\ \bar{u}_3 \\ \bar{u}_4 \\ \bar{u}_5 \\ \bar{u}_6 \\ \bar{u}_7 \\ \bar{u}_8 \end{array}\right\}$$

or

$$\boldsymbol{\epsilon}(\hat{x},\hat{y},t) = \boldsymbol{B}_{\mathrm{e}}(\hat{x},\hat{y})\ \bar{\boldsymbol{u}}(t)$$

6.2 Stress-Strain relationships

6.2.1 Plane-Stress

In-plane behavior of thin plates, $\sigma_{zz} = \tau_{xz} = \tau_{yz} = 0$
For plane-stress elasticity, the stress-strain relationship simplifies to

$$\left\{ \begin{array}{c} \sigma_{xx} \\ \sigma_{yy} \\ \tau_{xy} \end{array} \right\} = \frac{E}{1-\nu^2} \left[\begin{array}{ccc} 1 & \nu & 0 \\ \nu & 1 & 0 \\ 0 & 0 & \frac{1}{2}(1-\nu) \end{array} \right] \left\{ \begin{array}{c} \epsilon_{xx} \\ \epsilon_{yy} \\ \gamma_{xy} \end{array} \right\} \tag{106}$$

or

$$\boldsymbol{\sigma} = \boldsymbol{S}_{\mathrm{p}\sigma} \ \boldsymbol{\epsilon} \tag{107}$$

6.2.2 Plane-Strain

In-plane behavior of continua, $\epsilon_{zz} = \gamma_{xz} = \gamma_{yz} = 0$
For plane-strain elasticity, the stress-strain relationship simplifies to

$$\left\{ \begin{array}{c} \sigma_{xx} \\ \sigma_{yy} \\ \tau_{xy} \end{array} \right\} = \frac{E}{(1+\nu)(1-2\nu)} \left[\begin{array}{ccc} 1-\nu & \nu & 0 \\ \nu & 1-\nu & 0 \\ 0 & 0 & \frac{1}{2}-\nu \end{array} \right] \left\{ \begin{array}{c} \epsilon_{xx} \\ \epsilon_{yy} \\ \gamma_{xy} \end{array} \right\} \tag{108}$$

or

$$\boldsymbol{\sigma} = \boldsymbol{S}_{\mathrm{p}\epsilon} \ \boldsymbol{\epsilon} \tag{109}$$

6.3 2D Rectangular Element Mass Matrix

Consistent mass matrix

$$\bar{\boldsymbol{M}} = \int_0^1 \int_0^1 \ \left[\boldsymbol{\Psi}^{\mathsf{T}}(\hat{x},\hat{y}) \ \rho \ \boldsymbol{\Psi}(\hat{x},\hat{y}) \right]_{8\times 8} \ h \ a \ d\hat{x} \ b \ d\hat{y} \tag{110}$$

6.4 2D Rectangular Element Elastic Stiffness Matrix

Elastic element stiffness matrix

$$\bar{\boldsymbol{K}}_{\mathrm{e}} = \int_0^1 \int_0^1 \left[\boldsymbol{B}_{\mathrm{e}}^{\mathsf{T}}(\hat{x},\hat{y}) \ \boldsymbol{S}_{\mathrm{e}}(E,\nu) \ \boldsymbol{B}_{\mathrm{e}}(\hat{x},\hat{y}) \right]_{8\times 8} h \ a \ d\hat{x} \ b \ d\hat{y} \tag{111}$$

6.5 2D Rectangular Plane-Stress and Plane-Strain Element Stiffness and Mass Matrices

6.5.1 *Plane-Stress stiffness matrix*

$$\bar{\boldsymbol{K}}_{\rm e} = \frac{Eh}{12(1-\nu^2)} \cdot$$

$$\left[\begin{array}{cccccccc}
4c+k_A & k_B & -4c+k_A/2 & -k_C & -2c-k_A/2 & -k_B & 2c-k_A & k_C \\
k_B & 4/c+k_D & k_C & 2/c-k_D & -k_B & -2/c-k_D/2 & -k_C & -4/c+k_D/2 \\
-4c+k_A/2 & k_C & 4c+k_A & -k_B & 2c-k_A & -k_C & -2c-k_A/2 & k_B \\
-k_C & 2/c-k_D & -k_B & 4/c+k_D & k_C & -4/c+k_D/2 & k_B & -2/c-k_D/2 \\
-2c-k_A/2 & -k_B & 2c-k_A & k_C & 4c+k_A & k_B & -4c+k_A/2 & -k_C \\
-k_B & -2/c-k_D/2 & -k_C & -4/c+k_D/2 & k_B & 4/c+k_D & k_C & 2/c-k_D \\
2c-k_A & -k_C & -2c-k_A/2 & k_B & -4c+k_A/2 & k_C & 4c+k_A & -k_B \\
k_C & -4/c+k_D/2 & k_B & -2/c-k_D/2 & -k_C & 2/c-k_D & -k_B & 4/c+k_D
\end{array}\right]$$

where $c = b/a$ and

$$\begin{aligned}
k_A &= (2/c)(1-\nu) \\
k_B &= (3/2)(1+\nu) \\
k_C &= (3/2)(1-3\nu) \\
k_D &= (2c)(1-\nu)
\end{aligned}$$

6.5.2 *Plane-Strain stiffness matrix*

$$\bar{\boldsymbol{K}}_{\rm e} = \frac{Eh}{12(1+\nu)(1-2\nu)} \cdot$$

$$\left[\begin{array}{cccccccc}
k_A+k_B & 3/2 & -k_A+k_B/2 & 6\nu-3/2 & -k_A/2-k_B/2 & -3/2 & k_A/2-k_B & 3/2-6\nu \\
3/2 & k_C+k_D & 3/2-6\nu & k_C/2-k_D & -3/2 & -k_C/2-k_D/2 & 6\nu-3/2 & -k_C+k_D/2 \\
-k_A+k_B/2 & 3/2-6\nu & k_A+k_B & -3/2 & k_A/2-k_B & 6\nu-3/2 & -k_A/2-k_B/2 & 3/2 \\
6\nu-3/2 & k_C/2-k_D & -3/2 & k_C+k_D & 3/2-6\nu & -k_C+k_D/2 & 3/2 & -k_C/2-k_D/2 \\
-k_A/2-k_B/2 & -3/2 & k_A/2-k_B & 3/2-6\nu & k_A+k_B & 3/2 & -k_A+k_B/2 & 6\nu-3/2 \\
-3/2 & -k_C/2-k_D/2 & 6\nu-3/2 & -k_C+k_D/2 & 3/2 & k_C+k_D & 3/2-6\nu & k_C/2-k_D \\
k_A/2-k_B & 6\nu-3/2 & -k_A/2-k_B/2 & 3/2 & -k_A+k_B/2 & 3/2-6\nu & k_A+k_B & -3/2 \\
3/2-6\nu & -k_C+k_D/2 & 3/2 & -k_C/2-k_D/2 & 6\nu-3/2 & k_C/2-k_D & -3/2 & k_C+k_D
\end{array}\right]$$

where $c = b/a$ and

$$\begin{aligned}
k_A &= (4c)(1-\nu) \\
k_B &= (2/c)(1-2\nu) \\
k_C &= (4/c)(1-\nu) \\
k_D &= (2c)(1-2\nu)
\end{aligned}$$

6.5.3 Mass matrix

The element mass matrix for the plane-stress and plane-strain elements is the same.

$$\bar{\boldsymbol{M}} = \frac{\rho a b h}{36} \left[\begin{array}{cccccccc} 4 & 0 & 2 & 0 & 1 & 0 & 2 & 0 \\ 0 & 4 & 0 & 2 & 0 & 1 & 0 & 2 \\ 2 & 0 & 4 & 0 & 2 & 0 & 1 & 0 \\ 0 & 2 & 0 & 4 & 0 & 2 & 0 & 1 \\ 1 & 0 & 2 & 0 & 4 & 0 & 2 & 0 \\ 0 & 1 & 0 & 2 & 0 & 4 & 0 & 2 \\ 2 & 0 & 1 & 0 & 2 & 0 & 4 & 0 \\ 0 & 2 & 0 & 1 & 0 & 2 & 0 & 4 \end{array} \right] \tag{112}$$

Note, again, that these element stiffness matrices are approximations based on an assumed distribution of internal displacements.

7 Element damping matrices

Damping in vibrating structures can arise from diverse linear and nonlinear phenomena.

If the structure is in a fluid (liquid or gas), the motion of the structure is resisted by the fluid viscosity. At low speeds (low Reynolds numbers), this damping effect can be taken to be linear in the velocity, and the damping forces are proportional to the total rate of displacement (not the rate of deformation). If the fluid is flowing past the structure at high flow rates (high Reynolds numbers), the motion of the structure can interact with the flowing medium. This interaction affects the dynamics (natural frequencies and damping ratios) of the coupled structure-fluid system. Potentially, at certain flow speeds, the motion of the structure can increase the transfer of energy from the flow into the structure, giving rise to an aero-elastic instability.

Damping can also arise within structural systems from friction forces internal to the structure (the micro-slip within joints and connections) inherent material viscoelasticity, and inelastic material behavior. In many structural systems, a type of damping in which damping stresses are proportional to strain and in-phase with strain-rate are assumed. Such so-called "complex-stiffness damping" or "structural damping" is commonly used to model the damping in soils. Fundamentally, this kind of damping is neither elastic nor viscous. The force-displacement behavior does not follow the same path in loading and unloading, behavior but instead follows a "butterfly" shaped path. Nevertheless, this type of damping is commonly linearized as linear viscous damping, in which forces are proportional to the rate of deformation.

In materials in which stress depends on strain and strain rate, a Voigt viscoelasticity model may be assumed, in which stress is proportional to both strain $\boldsymbol{\epsilon}$ and strain-rate $\dot{\boldsymbol{\epsilon}}$,

$$\boldsymbol{\sigma} = [\ \boldsymbol{S}_{\rm e}(E,\nu)\ ]\ \boldsymbol{\epsilon} + [\ \boldsymbol{S}_{\rm v}(\eta)\ ]\ \dot{\boldsymbol{\epsilon}}$$

The internal virtual work of real viscous stresses $\boldsymbol{S}_{\rm v}\dot{\boldsymbol{\epsilon}}$ moving through virtual strains $\delta\boldsymbol{\epsilon}$ is

$$\begin{aligned}
\delta W_{\rm D} &= \int_V \boldsymbol{\sigma}^{\mathsf{T}}(\boldsymbol{x},t)\ \delta\boldsymbol{\epsilon}(\boldsymbol{x},t)\ dV \qquad (113)\\
&= \int_V \dot{\boldsymbol{\epsilon}}^{\mathsf{T}}(\boldsymbol{x},t)\ \boldsymbol{S}_{\rm v}(\eta)\ \delta\boldsymbol{\epsilon}(\boldsymbol{x},t)\ dV \\
&= \int_V \dot{\bar{\boldsymbol{u}}}^{\mathsf{T}}(t)\boldsymbol{B}_{\rm e}^{\mathsf{T}}(\boldsymbol{x})\ \boldsymbol{S}_{\rm v}(\eta)\ \boldsymbol{B}_{\rm e}(\boldsymbol{x})\delta\bar{\boldsymbol{u}}(t)\ dV \\
&= \dot{\bar{\boldsymbol{u}}}^{\mathsf{T}}(t)\ \int_V \Big[\boldsymbol{B}_{\rm e}^{\mathsf{T}}(\boldsymbol{x})\ \boldsymbol{S}_{\rm v}(\eta)\ \boldsymbol{B}_{\rm e}(\boldsymbol{x})\Big]_{N\times N} dV\ \delta\bar{\boldsymbol{u}}(t) \qquad (114)
\end{aligned}$$

Given a material viscous damping matrix, $\boldsymbol{S}_{\rm v}$, a structural element damping matrix can be determined for any type of structural element, through the integral in equation (114), as has been done for stiffness and mass element matrices earlier in this document. In doing so, it may be assumed that the internal element displacements $u_i(\boldsymbol{x},t)$ (and the matrices $[\boldsymbol{\Psi}]$ and $[\boldsymbol{B}]$) are unaffected by the presence of damping, though this is not strictly true. Further, the parameters in $\boldsymbol{S}_{\rm v}(\eta)$ are often dependent on the frequency of the strain and the strain amplitude. Damping behavior that is amplitude-dependent is outside the domain of linear analysis.

7.1 Rayleigh damping matrices for structural systems

In an *assembled* model for a structural system, a damping matrix that is proportional to system's mass and stiffness matrices is called a Rayleigh damping matrix.

$$\boldsymbol{C}_{\rm s} = \alpha\boldsymbol{M}_{\rm s} + \beta\boldsymbol{K}_{\rm s}$$

$$\bar{\boldsymbol{R}}^{\mathsf{T}}\boldsymbol{C}_{\rm s}\bar{\boldsymbol{R}} = \begin{bmatrix} 2\zeta_1\omega_{\rm n1} & & \\ & \ddots & \\ & & 2\zeta_N\omega_{{\rm n}N}\end{bmatrix} = \alpha\begin{bmatrix} 1 & & \\ & \ddots & \\ & & 1\end{bmatrix} + \beta\begin{bmatrix} \omega_{\rm n1}^2 & & \\ & \ddots & \\ & & \omega_{{\rm n}N}^2\end{bmatrix} \qquad (115)$$

where $\omega_{{\rm n}j}^2$ is an eigen-value (squared natural frequency) and the columns of $\bar{R}$ are mass-normalized eigen-vectors (modal vectors) of the generalized eigen-problem

$$[\boldsymbol{K}_{\rm s} - \omega_{{\rm n}j}^2\boldsymbol{M}_{\rm s}]\bar{\boldsymbol{r}}_j = \boldsymbol{0}\ . \qquad (116)$$

From equations (115) it can be seen that the damping ratios satisfy

$$\zeta_j = \frac{\alpha}{2}\frac{1}{\omega_{{\rm n}j}} + \frac{\beta}{2}\omega_{{\rm n}j}$$

and the Rayleigh damping coefficients (α and β) can be determined so that the damping ratios ζ_j have desired values at two frequencies. The damping ratios modeled by Rayleigh damping can get very large for low and high frequencies. Rayleigh damping grows to ∞ as $\omega \to 0$ and increases linearly with ω for large values of ω. Note that the Rayleigh damping matrix has the same banded form as the mass and stiffness matrices. In other words, with Rayleigh damping, internal damping forces are applied only between coordinates that are connected by structural elements.

7.2 Caughey damping matrices for structural systems

The Caughey damping matrix is a generalization of the Rayleigh damping matrix. Caughey damping matrices can involve more than two parameters and can therefore be used to provide a desired amount of damping over a range of frequencies. The Caughey damping matrix for an *assembled* model for a structural system is

$$\boldsymbol{C}_{\mathrm{s}} = \boldsymbol{M}_{\mathrm{s}} \sum_{j=n_1}^{j=n_2} \alpha_j (\boldsymbol{M}_{\mathrm{s}}^{-1} \boldsymbol{K}_{\mathrm{s}})^j$$

where the index range limits n_1 and n_2 can be positive or negative, as long as $n_1 < n_2$. As with the Rayleigh damping matrix, the Caughey damping matrix may also be diagonalized by the real eigen-vector matrix $\bar{\boldsymbol{R}}$. The coefficients α_j are related to the damping ratios, ζ_k, by

$$\zeta_k = \frac{1}{2}\frac{1}{\omega_k} \sum_{j=n_1}^{j=n_2} \alpha_j \omega_k^{2j}$$

The coefficients α_j may be selected so that a set of specified damping ratios ζ_k are obtained at a corresponding set of frequencies ω_k. If $n_1 = 0$ and $n_2 = 1$, then the Caughey damping matrix is the same as the Rayleigh damping matrix. For other values of n_1 and n_2 the Caughey damping matrix loses the banded structure of the Rayleigh damping matrix, implying the presence of damping forces between coordinates that are not connected by structural elements.

Structural systems with classical damping have real-valued modes $\bar{\boldsymbol{r}}_j$ that depend only on the system's mass and stiffness matrices (equation (116)), and can be analyzed as a system of uncoupled second-order ordinary differential equations. The responses of the system coordinates can be approximated via a modal expansion of a select subset of modes. The convenience of the application of modal-superposition to the transient response analysis of structures is the primary motivation

7.3 Rayleigh damping matrices for structural elements

An element Rayleigh damping matrix may be easily computed from the element's mass and stiffness matrix $\bar{\boldsymbol{C}} = \alpha\bar{\boldsymbol{M}} + \beta\bar{\boldsymbol{K}}$ and assembled into a damping matrix for the structural system $\boldsymbol{C}_{\mathrm{s}}$. The element damping is presumed to increases linearly with the mass and the stiffness of the element; larger elements will have greater mass, stiffness, and damping. System damping matrices assembled from such element damping matrices will have the same banding as the mass and stiffness matrices; internal damping forces will occur only between coordinates connected by a structural element. However, such an assembled damping matrix will not be diagonalizeable by the real eigenvectors of the structural system mass matrix $\boldsymbol{M}_{\mathrm{s}}$ and stiffness matrix $\boldsymbol{K}_{\mathrm{s}}$.

7.4 Linear viscous Damping elements

Some structures incorporate components designed to provide supplemental damping. These supplemental damping components can dissipate energy through viscosity, friction, or inelastic deformation. In a linear viscous damping element (a dash-pot), damping forces are linear in the velocity across the nodes of the element and the forces act along a line between the two nodes of the element. The element node damping forces $\bar{\boldsymbol{f}}_{\rm d}$ are related to the element node velocities $\bar{\boldsymbol{v}}_{\rm d}$ through the damping coefficient $c_{\rm d}$

$$\begin{bmatrix} \bar{f}_{\rm d1} \\ \bar{f}_{\rm d2} \end{bmatrix} = \begin{bmatrix} c_{\rm d} & -c_{\rm d} \\ -c_{\rm d} & c_{\rm d} \end{bmatrix} \begin{bmatrix} \bar{v}_{\rm d1} \\ \bar{v}_{\rm d2} \end{bmatrix}$$

The damping matrix for a linear viscous damper connecting a node at (x_1, y_1) to a node at (x_2, y_2) is found from the element coordinate transformation,

$$\boldsymbol{C}_{6\times 6} = \begin{bmatrix} c & s & 0 & 0 & 0 & 0 \\ 0 & 0 & 0 & c & s & 0 \end{bmatrix}^{\sf T} \begin{bmatrix} c_{\rm d} & -c_{\rm d} \\ -c_{\rm d} & c_{\rm d} \end{bmatrix} \begin{bmatrix} c & s & 0 & 0 & 0 & 0 \\ 0 & 0 & 0 & c & s & 0 \end{bmatrix}$$

where $c = (x_2 - x_1)/L$ and $s = (y_2 - y_1)/L$. Structural systems with supplemental damping components generally have non-classical system damping matrices.

8 Assembly of Structural System Matrices

The method by which structural element matrices are assembled into structural system matrices is called *matrix assembly*. The types of information required for matrix assembly is represented via the example shown in Figure 13. This model has seven nodes and eighteen coordinates. Eight coordinates are reaction coordinates which rigidly prevent displacements in their directions.

The procedure for matrix assembly follows these steps.

1. List the model information:
   - node coordinates (x_i, y_i) for each node
     - In this example, $(x_3, y_3) = (675, 525)$, $(x_6, y_6) = (400, 0)$, etc.
   - element connectivity for each element.
     The connectivity data indicates the set of nodes connected by each element.
     Bar and beam elements have two nodes.
     The 2D elastic element in this example has four nodes.
     In this example,
     - the connectivity for the one bar element is: $(n_{11}, n_{21}) = (1, 2)$;
     - the connectivity for the three beam elements is:
       $(n_{11}, n_{21}) = (2, 3)$, $(n_{12}, n_{22}) = (3, 4)$, $(n_{13}, n_{23}) = (4, 5)$;

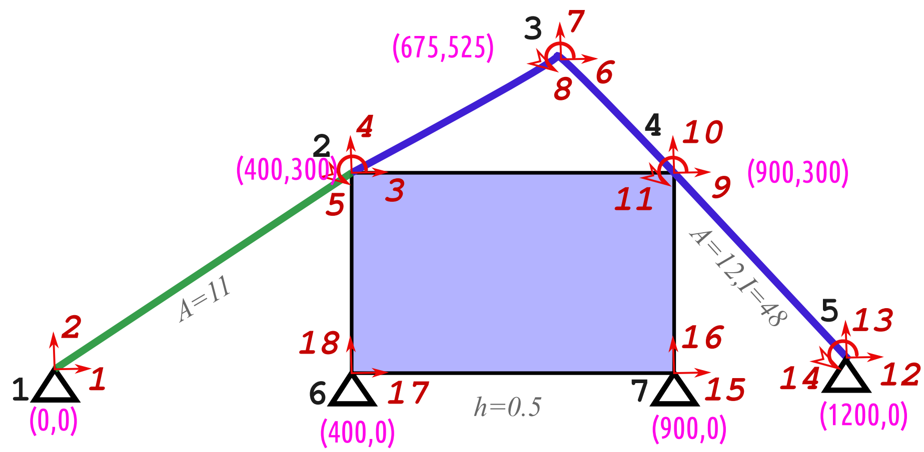

Figure 13. A model of a structural system represented by one bar element (green), three beam elements (blue), and one rectangular plate element (light blue). Structural node numbers are indicated in black; structural coordinates are indicated in red; node coordinates are indicated in magenta; element cross section properties are indicated in grey; pinned (reaction) nodes are indicated as triangles. All dimensional values are in units of mm, mm^2, mm^4. The material is Aluminum (2024).

   - the connectivity for the one plate element is: $(n_{11}, n_{21}, n_{31}, n_{41}) = (4, 2, 6, 7)$.

- the material and cross section properties of each element.
   - for bar elements the relevant information is elastic modulus E, mass density ρ, and cross section area A;
   - for Bernoulli-Euler beam elements the relevant information is elastic modulus E, mass density ρ, cross section area A, and bending moment of inertia I;
   - for 2D elastic elements, the relevant information is elastic modulus E, mass density ρ, Poisson's ratio ν, and thickness h.

2. For each element (one bar, three beams, one 2D elastic element in this example), compute the element matrices (for stiffness, mass, and damping) in their local coordinates. This involves determining the dimensions of the elements (for bars and beams the dimension is the length L, for 2D elastic elements the dimensions are a and b) from the element's node locations.

   - bar element matrices in local element coordinates are given in sections 2.3 and 2.2
   - Bernoulli-Euler beam element matrices in local element coordinates are given in section 3.6
   - 2D elastic element matrices in local element coordinates are given in section 6.5

3. Transform the element matrices for their local coordinates to their global coordinates via the coordinate transformation matrix $\boldsymbol{T}$, which depends on the angle of the element, which can be found from the element coordinates as described in section 5.2 and 5.3. Element damping matrices in global coordinates $\bar{\boldsymbol{C}}$ can be approximated by the Rayleigh Damping method, in which $\bar{\boldsymbol{C}} = \alpha\bar{\boldsymbol{M}} + \beta\bar{\boldsymbol{K}}$

   At this point in the process element stiffness, mass, and damping matrices have been determined for each element.

4. System Matrix Assembly

   The matrix assembly process makes use of the correspondence between the element coordinates in the global directions to the structural coordinates (shown in red in Figure 13)

5. For the one bar element: $(n_{11}, n_{21}) = (1, 2)$, Coordinates 1 and 2 of the bar correspond to coordinates 1 and 2 of the structure. Coordinates 3 and 4 of the bar correspond to coordinates 3 and 4 of the structure. The correspondence vector between the four bar element coordinates and the structure coordinates, is therefore $c = (1, 2, 3, 4)$

6. For the three beam elements:
   $(n_{11}, n_{21}) = (2, 3)$, with the coordinate correspondence vector $c = (3, 4, 5, 6, 7, 8)$
   $(n_{12}, n_{22}) = (3, 4)$, with the coordinate correspondence vector $c = (6, 7, 8, 9, 10, 11)$
   $(n_{13}, n_{23}) = (4, 5)$; with the coordinate correspondence vector $c = (9, 10, 11, 12, 13, 14)$

7. the one 2D elastic element: $(n_{11}, n_{21}, n_{31}, n_{41}) = (4, 2, 6, 7)$. with the coordinate correspondence vector $c = (9, 10, 3, 4, 17, 18, 15, 16)$

   Structural analysis software takes care of numbering the structural coordinates, and establishing the coordinate correspondence vectors for each element. This task becomes somewhat complicated in software that incorporates elements with different numbers of element coordinates, e.g., software that includes bars and beams and dampers and 2D elastic elements.

   With the coordinate correspondence vectors established for each element, the element matrices may now be *assembled* into the correct indices of the structural system matrices.

   The values in each element matrix are assembled into the rows c and columns c of the corresponding system matrix. To start with, the structural system mass, stiffness, and damping matrices $(\boldsymbol{M}_s, \boldsymbol{K}_s, \boldsymbol{C}_s)$ are initialized to zero. In this example, these three system matrices are all 18-by-18.

   - For the one bar, the 4-by-4 matrices will add into coordinates (1,2,3,4) of the structural system matrix.

- For the three beams:
  the 6-by-6 matrices for the first beam will add into coordinates (3,4,5,6,7,8) of the structural system matrix.
  the 6-by-6 matrices for the second beam will add into coordinates (6,7,8,9,10,11) of the structural system matrix.
  the 6-by-6 matrices for the third beam will add into coordinates (9,10,11,12,13,14) of the structural system matrix.
- for the one 2D elastic element, the 8-by-8 matrices will add into coordinates (9, 10, 3, 4, 17, 18, 15, 16) of the structural system matrices

  Taking the assembly of the 2D elastic stiffness element matrices into the system stiffness matrix in more detail,

  - $\boldsymbol{K}_{1,1}$ for the element adds into $\boldsymbol{K}_{s\ 9,9}$ for the system.
  - $\boldsymbol{K}_{1,2}$ for the element adds into $\boldsymbol{K}_{s\ 9,10}$ for the system.
  - $\boldsymbol{K}_{1,7}$ for the element adds into $\boldsymbol{K}_{s\ 9,15}$ for the system.
  - $\boldsymbol{K}_{1,8}$ for the element adds into $\boldsymbol{K}_{s\ 9,16}$ for the system.
  - $\boldsymbol{K}_{2,6}$ for the element adds into $\boldsymbol{K}_{s\ 10,18}$ for the system.
  - $\boldsymbol{K}_{5,1}$ for the element adds into $\boldsymbol{K}_{s\ 17,9}$ for the system.
  - $\boldsymbol{K}_{5,4}$ for the element adds into $\boldsymbol{K}_{s\ 17,4}$ for the system.
  - $\boldsymbol{K}_{7,8}$ for the element adds into $\boldsymbol{K}_{s\ 15,16}$ for the system.
  - $\boldsymbol{K}_{8,8}$ for the element adds into $\boldsymbol{K}_{s\ 16,16}$ for the system.

```
% assemble matrices for rectangular 2D element number "r" into the system matrices

    n1 = REN(1,r);                         % rectangular element node 1
    n2 = REN(2,r);                         % rectangular element node 2
    n3 = REN(3,r);                         % rectangular element node 3
    n4 = REN(4,r);                         % rectangular element node 4

    x1 = XY(1,n1);  y1 = XY(2,n1);         % coordinates of node 1
    x2 = XY(1,n2);  y2 = XY(2,n2);         % coordinates of node 2
    x3 = XY(1,n3);  y3 = XY(2,n3);         % coordinates of node 3
    x4 = XY(1,n4);  y4 = XY(2,n4);         % coordinates of node 4

    % compute the three 8-by-8 stiffness, mass, and damping matrices
    % for the rectangular 2D elements
    [Ke,Me,Ce,A(p)] = rectangular_element(x1,y1,x2,y2,x3,y3,x4,y4,Evtpab(:,r),PS);

    % coordinate coorespondence vector for the 2D elastic element in this example
    % in general, this vector would be established within the software
    cc = [ 9, 10, 3, 4, 17, 18, 15, 16 ];  % *** for this example ***

    Ks(cc,cc) = Ks(cc,cc) + Ke;                    % matrix assembly
    Ms(cc,cc) = Ms(cc,cc) + Me;                    % matrix assembly
    Cs(cc,cc) = Cs(cc,cc) + Ce;                    % matrix assembly
```

9 Solving for the Static Equilibruim of Geometrically Nonlinear Structures

In structural analysis, if deformations are negligibly small (or *infinitesimal*) analyzing equilibrium in the undeformed configuration provides sufficiently accurate results. If deformations are not negligible, (i.e., if they are *finite*) equilibrium should be analyzed in the deformed configuration.

Finite deformation analysis is always more accurate than small deformation analysis, and when strains are large ($> 0.05\%$) the increased accuracy may be significant. Further, finite deformation analysis may be used to analyze buckling potential of structures.

In finite deformation analysis the stiffness depends on the element stresses. For beams and bars, the stiffness depends on axial forces. One needs to know the element tensions in order to compute the stiffness but one needs the stiffness to compute the tensions. The solution to such problems is to proceed incrementally by increasing deformations in steps until equilibrium is achieved for the specified loads, in the deformed configuration, and with the desired precision. Two algorithms for step-by-step deformation are described later in this document.

The element stiffness matrix may be separated into an elastic part, $\bar{\boldsymbol{K}}_{\mathrm{e}}$, and a *geometric* part, $\bar{\boldsymbol{K}}_{\mathrm{g}}$ that accounts for the effects of finite deformation.

9.1 Tension Forces

We may compute the tension force in terms of the four end displacements, $\bar{u}_1$, $\bar{u}_2$, $\bar{u}_4$, and $\bar{u}_5$. The tension force is approximated by $T \approx (EA/L_o)\Delta$, where the stretch in the bar, Δ, is found from the four end displacements, $\bar{u}_1$, $\bar{u}_2$, $\bar{u}_4$, and $\bar{u}_5$.

$$\begin{aligned} (L_o + \Delta)^2 &= (L_o + \bar{u}_4 - \bar{u}_1)^2 + (\bar{u}_5 - \bar{u}_2)^2 \\ L_o^2 + 2L_o\Delta + \Delta^2 &= L_o^2 + \bar{u}_4^2 + \bar{u}_1^2 + 2L_o\bar{u}_4 - 2L_o\bar{u}_1 - 2\bar{u}_4\bar{u}_1 + (\bar{u}_5 - \bar{u}_2)^2 \\ 2L_o\Delta + \Delta^2 &= 2L_o(\bar{u}_4 - \bar{u}_1) + (\bar{u}_4 - \bar{u}_1)^2 + (\bar{u}_5 - \bar{u}_2)^2 \end{aligned}$$

This is a quadratic equation in Δ. Limiting strains to the elastic range of metals, $|\Delta/L_o| < 0.002$ so $|\Delta^2/(2L_o\Delta)| < 0.001$, and the Δ^2 term can be neglected. This leads to the approximation

$$\Delta \approx (\bar{u}_4 - \bar{u}_1) + \frac{1}{2L_o}(\bar{u}_4 - \bar{u}_1)^2 + \frac{1}{2L_o}(\bar{u}_5 - \bar{u}_2)^2 \ , \tag{117}$$

which provides a relation for Δ that is not quite as complicated as the quadratic formula. The first term in parenthesis is the stretch considering infinitesimal deformations; the second and third terms are the contribution of the finite deformation effects. Optionally the $(\bar{u}_4 - \bar{u}_1)^2$ term can be neglected, since axial displacements are much smaller than transverse displacements. This approximation is typically accurate to within to within 0.0001% to 0.001% for strains up to 0.1%, which is on the order of the yield strain of most metals. The tension in a bar, including finite deformation effects, is

$$T \approx \frac{EA}{L_o} \left[(\bar{u}_4 - \bar{u}_1) + \frac{1}{2L_o} (\bar{u}_5 - \bar{u}_2)^2 \right] , \tag{118}$$

In general, for trusses with metallic elements that are stressed to near their yield stress (axial strains $\approx 0.1\%$), geometric stiffness effects can affect node displacements by a fraction of a percent and can affect bar forces by a few percent. Trusses made of stronger or more flexible materials, such as plastics with elastic strains reaching 1% to 5%, geometric stiffness effects can be much more significant. Furthermore, geometric stiffness effects can be more significant in frames than in trusses.

The following approximations are invoked in finite strain analysis:

- Coordinate transformations $\boldsymbol{T}$ are independent of the deformation (error $\approx 0.1\%$);
- $(T/L) \approx (T/L_o)$ . . . so that $\bar{\boldsymbol{K}}_{\rm g}$ depends on $\bar{u}$ only through T (error $\approx 0.0001\%$ to 0.001%);
- Tension forces $T \approx \frac{EA}{L_o} \left[(\bar{u}_4 - \bar{u}_1) + \frac{1}{2L_o} (\bar{u}_5 - \bar{u}_2)^2 \right]$ . . . so that T can be found without computing quadratic roots or logarithms (error $\approx 0.0001\%$ to 0.001%).

Only the first approximation is required for the stiffness matrix assembly process. The other approximations merely simplify the calculations. However, the effects of these approximations for strains less than 1% are truly minuscule.

9.2 Solving Nonlinear Problems using Newton-Raphson and Broyden Methods

Recall the truncated Taylor series expansion of a nonlinear function $\boldsymbol{f}(\boldsymbol{x})$,

$$\boldsymbol{f} - \boldsymbol{f}_o = \left[\frac{\partial \boldsymbol{f}}{\partial \boldsymbol{x}} \right] (\boldsymbol{x} - \boldsymbol{x}_o) \ + \ \text{h.o.t.} \ .$$

To solve a system of nonlinear equations $\boldsymbol{f}(\boldsymbol{x}_o) = \boldsymbol{f}_o$ for the vector of unknowns $\boldsymbol{x}_o$, we may proceed in an incremental fashion, by first evaluating $\boldsymbol{f}^{(i)} = \boldsymbol{f}(\boldsymbol{x}^{(i)})$ for a trial vector $\boldsymbol{x}^{(i)}$. If we know the *Jacobian matrix* $[\partial \boldsymbol{f} / \partial \boldsymbol{x}]$ evaluated at the vector $\boldsymbol{x} = \boldsymbol{x}^{(i)}$, then the next trial value of the unknown vector should be

$$\boldsymbol{x}^{(i+1)} = \boldsymbol{x}^{(i)} - \left[\frac{\partial \boldsymbol{f}}{\partial \boldsymbol{x}} \right]^{-1}_{\boldsymbol{x}=\boldsymbol{x}^{(i)}} (\boldsymbol{f}^{(i)} - \boldsymbol{f}_o)$$

This is the essence of the Newton-Raphson method for solving sets of nonlinear equations. In the problem of finite deformation analysis of structures, the *equilibrium condition* is represented by a system of non-linear algebraic equations

$$\boldsymbol{f}(\boldsymbol{d}) = \boldsymbol{K}_{\rm s}(\boldsymbol{d}) \ \boldsymbol{d} \ ,$$

where the structural stiffness matrix $\boldsymbol{K}_{\rm s}(\boldsymbol{d})$ includes geometric stiffness effects, which depend on the bar tensions, T, which, in turn depend on the displacements, $\boldsymbol{d}$. In other words, $\boldsymbol{K}_{\rm s}(\boldsymbol{d})$ is a matrix that depends on the unknown displacements, $\boldsymbol{d}$. Note that the Jacobian matrix of this problem is $[\partial \boldsymbol{f}/\partial \boldsymbol{d}]$, which is not equal to $\boldsymbol{K}_{\rm s}(\boldsymbol{d})$. An explicit expression for the Jacobian $[\partial \boldsymbol{f}/\partial \boldsymbol{f}]$ is extremely difficult to derive but we can approximate it using a numerical technique. There are many ways to approximate an unknown Jacobian, and two approaches will be described here.

In the first approach, we use the structural stiffness matrix, $\boldsymbol{K}_{\rm s}$, as if it were the Jacobian matrix. In this approach, the iterations proceed as follows:

1. Initialize the displacements and bar tensions to be zero, $\boldsymbol{d}^{(0)} = \mathbf{0}$.
2. Assemble the structural stiffness matrix, for the initial configuration with zero displacements and zero bar tensions. Call this matrix $\boldsymbol{K}_{\rm s}^{(0)} = \boldsymbol{K}_{\rm s}(\boldsymbol{d}^{(0)})$.
3. Find the first approximation to the displacements, $\boldsymbol{d}^{(1)}$, by solving $\boldsymbol{f} = \boldsymbol{K}_{\rm s}^{(0)}\boldsymbol{d}^{(1)}$.
4. With these displacements, find the tension forces, including finite deformation effects, using equation.
5. Re-compute the structural stiffness matrix using this set of tension forces for deflections $\boldsymbol{d} = \boldsymbol{d}^{(1)}$, $\boldsymbol{K}_{\rm s}^{(1)} = \boldsymbol{K}_{\rm s}(\boldsymbol{d}^{(1)})$.
6. Go back to step 3, and continue to iterate until $||\boldsymbol{f} - \boldsymbol{K}_{\rm s}^{(i-1)}\boldsymbol{d}^{(i)}|| < \epsilon$ where ϵ is the convergence tolerance for the equilibrium error, or until you get tired of iterating.

In principle, this approach will converge to the correct solution for both stiffening systems and softening systems. The stiffness matrix at equilibrium, $\boldsymbol{K}_{\rm s}^{(n)}$, is symmetric and can be used for dynamic analysis of the structure under the effects of significant element tension forces. However, this approach can be slow to converge, and may not converge at all if the force displacement relation has an inflection point.

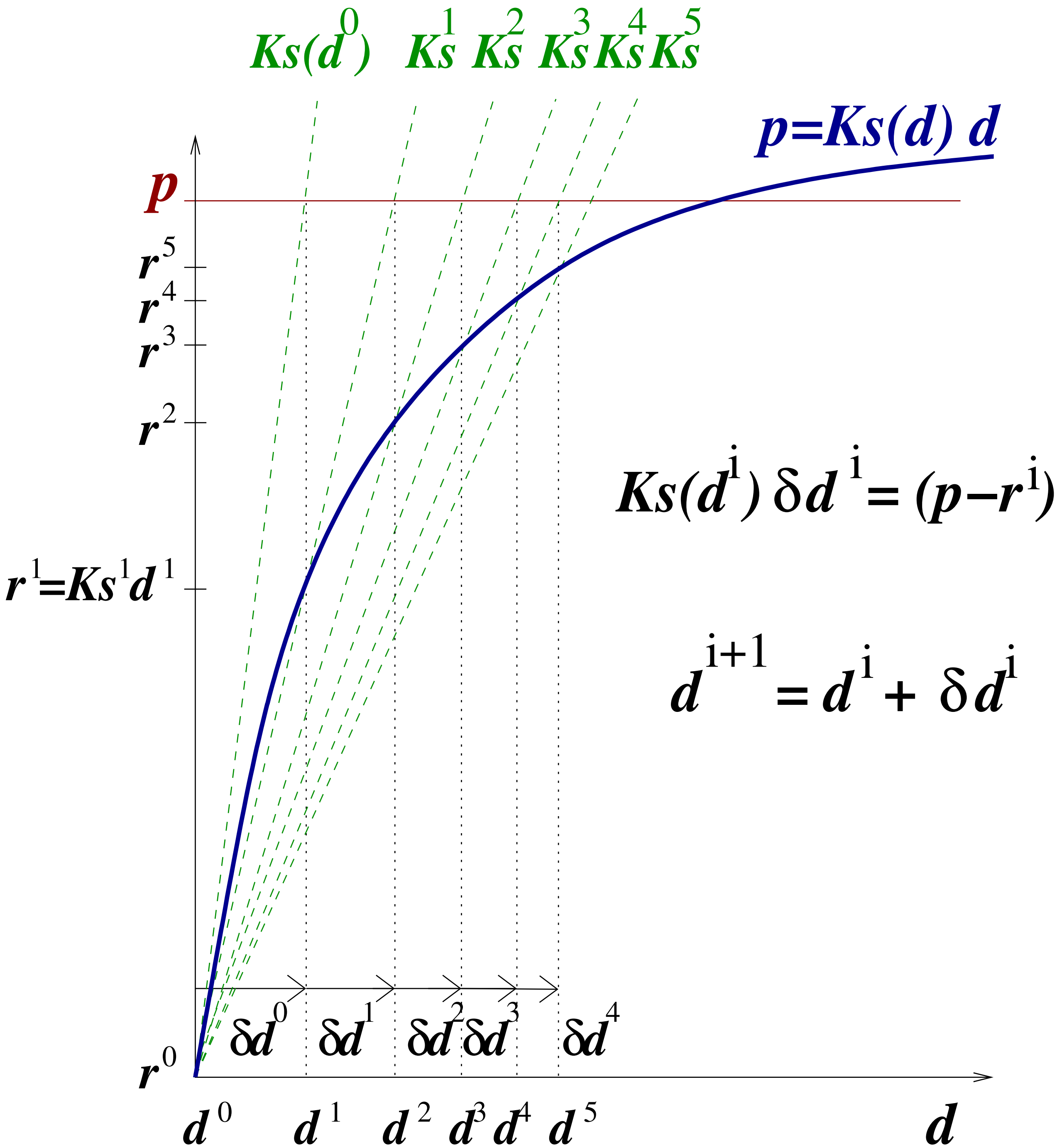

Figure 14. Modified Newton Raphson Method.

In the second approach, the Jacobian matrix, which is also called the *tangent stiffness matrix*,[1] is approximated by a *secant stiffness matrix*, for which we will use the symbol $\tilde{\boldsymbol{K}}_{\mathrm{s}}$. The

[1] Can you guess why?

secant stiffness matrix will be calculated using a technique attributed to C.G. Broyden.[2,3] In each iteration with the secant stiffness approach, we find incremental displacements, $\delta \boldsymbol{d}$, and add those displacements to the previously computed displacements. The procedure using Broyden's secant stiffness matrix is as follows:

1. Initialize the displacements and bar tensions to be zero, $\boldsymbol{d}^{(0)} = \boldsymbol{0}$.
2. Assemble the structural stiffness matrix, for the initial configuration with zero displacements and zero bar tensions, call this matrix $\boldsymbol{K}_{\rm s}^{(0)} = \boldsymbol{K}_{\rm s}(\boldsymbol{d}^{(0)})$. This matrix will also be the initial secant stiffness matrix, $\tilde{\boldsymbol{K}}_{\rm s}^{(0)} = \boldsymbol{K}_{\rm s}^{(0)}$. [4]
3. Find the first incremental displacements, $\delta \boldsymbol{d}^{(0)}$, by solving $\boldsymbol{f} = \boldsymbol{K}_{\rm s}^{(0)} \ \delta \boldsymbol{d}^{(0)}$.
4. Add these displacements to the initial displacements, $\boldsymbol{d}^{(0)}$, (which are zero), $\boldsymbol{d}^{(1)} = \boldsymbol{d}^{(0)} + \delta \boldsymbol{d}^{(0)} = \delta \boldsymbol{d}^{(0)}$.
5. With the displacements $\boldsymbol{d}^{(1)}$ find the tension forces, including finite deformation effects.
6. Compute the structural stiffness matrix, $\boldsymbol{K}_{\rm s}^{(1)} = \boldsymbol{K}_{\rm s}(\boldsymbol{d}^{(1)})$ using the set of tension forces for deflections $\boldsymbol{d}^{(1)}$, and compute the equilibrium error $\boldsymbol{f} \ - \ \boldsymbol{K}_{\rm s}^{(1)} \ \boldsymbol{d}^{(1)}$
7. Update the secant stiffness matrix using Broyden's formula.[5]
$$\tilde{\boldsymbol{K}}_{\rm s}^{(1)} = \tilde{\boldsymbol{K}}_{\rm s}^{(0)} - \frac{(\boldsymbol{f} - \boldsymbol{K}_{\rm s}^{(1)} \boldsymbol{d}^{(1)}) \times \delta \boldsymbol{d}^{(0)}}{\delta \boldsymbol{d}^{(0)} \cdot \delta \boldsymbol{d}^{(0)}}$$
The *times* symbol ($\times$) represents the vector outer product, which results in a matrix, and the *dot* ($\cdot$) represents the vector inner product, which results in a scalar.
8. Using this secant stiffness matrix, find the next set of incremental displacements, $\delta \boldsymbol{d}^{(1)}$.
$$\tilde{\boldsymbol{K}}_{\rm s}^{(1)} \ \delta \boldsymbol{d}^{(1)} = \boldsymbol{f} - \boldsymbol{K}_{\rm s}^{(1)} \boldsymbol{d}^{(1)}$$
9. Add the incremental displacements, $\delta \boldsymbol{d}^{(1)}$ to the current displacements, $\boldsymbol{d}^{(1)}$,
$$\boldsymbol{d}^{(2)} = \boldsymbol{d}^{(1)} + \delta \boldsymbol{d}^{(1)}$$
10. Increment the iteration counter, $i = i + 1$, return to step 6, and continue to iterate until the equilibrium error is sufficiently small, $||\boldsymbol{f} - \boldsymbol{K}_{\rm s}^{(i)} \ \boldsymbol{d}^{(i)}|| < \epsilon$.

Note that the secant stiffness matrix as computed by Broyden's method is not symmetric which limits its usefulness in other aspects of the modeling. The following diagram illustrates Newton-Raphson iterations using Broyden's secant stiffness approach. It is not hard to see how this approach can be substantially more efficient than the first approach.

[2] Press, W.H., et. al, *Numerical Recipes in C*, Cambridge, 1992, section 9.7

[3] Broyden, C.G., "A class of methods for solving simultaneous nonlinear equations," *Mathematics of Computation,* vol. 19, no. 92 1965, pp. 577–593.

[4] This is a good idea. Can you see why?

[5] Press, W.H., et. al, *Numerical Recipes in C*, Cambridge Univ. Press, 1992, section 9.7.

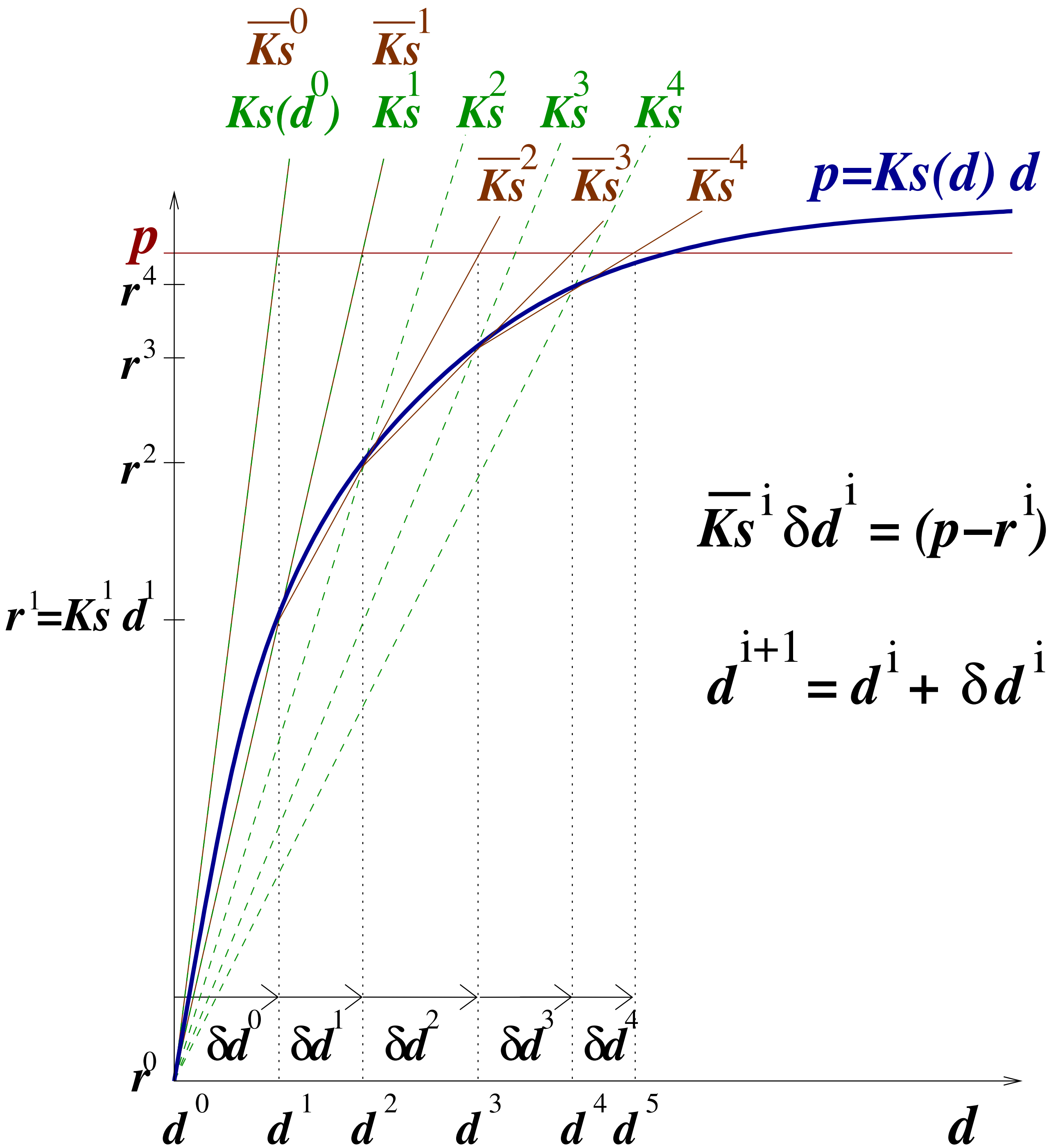

Figure 15. Modified Newton Raphson Method with Broyden secant stiffness updating.

10 Frame3DD: Static and Dynamic Analysis of 2D and 3D Frames.

Much of the contents of these notes are implemented in the open-source software, Frame3DD. http://frame3dd.sourceforge.net/

References

[1] Clough, Ray W., and Penzien, Joseph, *Dynamics of Structures,* 2nd ed. (revised), Computers and Structures, 2003.

[2] Cowper, G.R., "Shear Coefficient in Timoshenko Beam Theory," *J. Appl. Mech.,* 33(2)(1966):335-346

[3] Dong, S.B, Alpdogan, C., and Taciroglu, E. "Much ado about shear correction factors in Timoshenko beam theory," *Int. J. Solids & Structures,* 47(2010):1651-1655.

[4] Gruttman, F., and Wagner, W., "Shear correction factors in Timoshenko's beam theory for arbitrary shaped cross-sections," *Comp. Mech.* 27(2001):199-207.

[5] Kaneko, T., "An experimental study of the Timoshenko's shear coefficient for flexurally vibrating beams," J. Phys. D: Appl. Phys. 11 (1978): 1979-1988;

[6] Paz, Mario, *Structural Dynamics Theory and Computation,* Chapman & Hall, 2000.

[7] Przemieniecki, J.S., *Theory of Matrix Structural Analysis,* Dover, 1985. ⋆

[8] Rosinger, H.E., and Ritchie, I.G., "On Timoshenko's correction for shear in vibrating isotropic beams," *J. Phys. D: Appl. Phys.,* 10 (1977): 1461–1466.